2018

The Contribution of SARM1 to axonal degeneration in CNS inflammatory disorders

Daniel C. Njoku

Virginia Commonwealth University

The Contribution of SARM1 to axonal degeneration in CNS inflammatory disorders

A thesis submitted for partial fulfillment for the degree of Master of Science in the department of Physiology and Biophysics at Virginia Commonwealth University

By

DANIEL C. NJOKU

Cornell University, B.A. Chemistry, 2015

Principal Investigator: Unsong Oh, M.D.

Department of Neurology

Virginia Commonwealth University

Richmond, VA

May 2018

Table of Contents

Acknowledgments

First, I would like to thank my advisor and mentor for this project, Dr. Unsong Oh. I had my first research opportunity at Cornell University in the Department of Entomology, an experience that, I believe, furthered my passion for problem-solving with the scientific method. I came to VCU after graduation looking for a lab that I can apply myself and grow as a scientist. Dr. Oh asked me to join his lab in May 2016 for an opportunity to learn and to enhance my lab technical skills. Since then, he has not only been a gracious and kind mentor and an example of professionalism, he has helped me to see my real potential as a scientific thinker. Whether it was with animal dissection, PCR, or any of the numerous techniques I learned in his lab, Dr. Oh emphasized that I have patience and confidence in myself. I am indebted to him for his support, wisdom, and advice he has given me over the past 2 years. Even while he is taking care of patients, he has always made time for his students. He has certainly helped me get farther I ever hoped and I thank him for allowing me to work his lab for my master's degree. Because of my experiences in Dr. Oh's lab, I have a renewed passion for continuing with research in the future, using my knowledge that I have gained and will gain to help others in medicine.

I am also grateful to Dr. Jeff Dupree and Dr. Javier Maeso, two brilliant professors that graciously agreed to serve on my committee. The advice and guidance that you have given me from the time you accepted my request until now have helped move this project forward, and I am very grateful for your expertise and insights.

Finally, I would like to thank my parents and family for their support during this whole project.

Abbreviations:

AP-1- Activator protein 1

ASK- Apoptosis-signaling kinase

AXF GAM- Alexa Flour goat anti-mouse

AXF GARb- Alexa Flour goat anti-rabbit

AXF GARt- Alexa Flour goat anti-rat

BCL-XL- B-cell lymphoma extra large

BBB- Blood brain barrier

BSA- Bovine serum albumin

CARt-HRP- Chicken anti-rat IgG conjugated to horse radish peroxidase

CD- Cluster of differentiation

CFA- Complete Freund's adjuvant

DAM-HRP- Donkey anti-mouse IgG conjugated to horse radish peroxidase

DARb-HRP- Donkey anti- rabbit IgG conjugated to horse radish peroxidase

EAE- Experimental allergic encephalomyelitis

FGF- Fibroblast growth factor

HLA- Human leukocyte antigen

ICC- Immunocytochemistry

IHC- Immunohistochemistry

JNK- c-Jun N-terminal kinases

KA- Kainic acid

MAPK- Mitogen associated protein kinase

MBP- Myelin basic protein

MHC- Major histocompatibility complex

MKK4- Mitogen-activated protein kinase kinase 4

MMP- Matrix metalloproteases

MOG_{33-55}- Myelin oligodendrocyte glycoprotein peptide 33-55

mRNA – Messenger ribonucleic acid

NAD- Nicotinamide adenine dinucleotide

NAWN- Normal-appearing white matter

NMN- Nicotinamide mononucleotide

PBS- Phosphate buffered saline

PCR – Polymerase chain reaction

PDGF- β- Platelet-derived growth factor- beta

PECAM- Platelet/endothelial cell adhesion molecule

PHR- PAM-Highwire-Rpm-1

PIC- Protease inhibitor cocktail

PLP- Proteolipid protein

PP2A- Protein phosphatase 2

PPWM- Peri plaque white matter

ROS- Reactive oxygen species

RGC- Retinal ganglion cell

RIPA- Radio immunoprecipitation assay

TBS- Tris-buffered saline

TLR- Toll-like receptor

TGF-β- Transforming growth factor-beta

SNP- Single nucleotide polymorphism

Abstract

THE CONTRIBUTION OF SARM1 TO AXONAL DEGENERATION IN CNS INFLAMMATORY DISORDERS

By: Daniel C. Njoku, B.A.

A thesis submitted for partial fulfillment for the degree of Master of Science in the department of Physiology and Biophysics at Virginia Commonwealth University

Virginia Commonwealth University, 2018

Major director: Unsong Oh, M.D., Associate Professor, Department of Neurology

BACKGROUND: Multiple sclerosis (MS) is an inflammatory disease of the central nervous system (CNS) that results in demyelination and axonal loss. Efficiently targeting mechanisms of axonal degeneration in MS has the potential to reduce disability but remains an unmet need. Prior research has identified the protein sterile alpha and TIR motif containing 1 (SARM1) as a critical factor that promotes axonal destruction in the program of axonal degeneration known as Wallerian degeneration. SARM1 inactivation reduces axonal degeneration in a variety of contexts including traumatic and toxic injury, but it remains unknown to what extent SARM1 is involved in axonal degeneration triggered by CNS inflammation. METHODS: To test the hypothesis that SARM1 inactivation will reduce the burden of axonal degeneration associated with CNS inflammatory disorders, we first induced mice to have EAE and compared inflammation (CD3) and axonal damage (SMI-31/32, Beta APP) as compared to healthy control mice. We then studied experimental allergic encephalomyelitis (EAE) in *Sarm1* knockout (KO) and wild type (WT) mice. We used mice hemizygous for the Thy1-*YFP* transgene to study axonal damage. Degenerating axons were identified by focal swelling or fragmentation. Beta-

APP was also used as a marker of axonal injury. RESULTS: EAE mice had greater inflammation and axonal injury as compared to healthy mice. *Sarm1* KO mice are susceptible to developing EAE, with incidence comparable to WT littermates. Analysis of YFP^+ axons and Beta-APP showed that *Sarm1* KO mice had axonal damage reduced compared to WT littermates. CONCLUSION: *Sarm1* is highly expressed in the brain. Preliminary data suggest that SARM1 inactivation may minimize axonal degeneration in CNS inflammatory disorders such as EAE. Further studies are needed to confirm the long-term benefit.

INTRODUCTION

Epidemiology

MS is a nervous system disease that results in demyelination and axonal loss, which can lead to many devastating effects and a drastic adjustment in lifestyle for those who suffer from the disease. The prevalence of MS is highest in the continents of Europe and North America, with a prevalence rate of over 50 per 100,000 people, while it is lowest in South America and Africa, with a prevalence of less than 5 per 100,000 people (1). In recent years, MS has increased in prevalence worldwide. A 2013 report by the Multiple Sclerosis International Foundation (MSIF) and the World Health Organization (WHO) states that the number of people with MS increased from 2.1 million to 2.3 million (2). The reported increase in prevalence is due to factors such as an increase in survival rates of those who have the disease due to improved health care(2). MS ends up being very costly to patients specifically and to society at large. According to systematic reviews of MS costs, drug costs are the primary reason for high price among those who are dealing with a benign form of the disease, while those who are suffering from a more severe form has more of the cost contained in indirect expenses, such as lost productivity from missing work and school (3) (4). MS decreases the lifespan by about an average of 10 years (5) (6), but mortality rates for those who have MS have been declining over the last couple of decades because of improvement in treatment (5) (7). Other chronic diseases such as depression and diabetes have been associated with increasing the chance of mortality from MS (5).

Etiology

MS is an autoimmune disease of the CNS based on genetic and experimental evidence suggesting that both T-cells and B-cells may have roles in causing the phenotype through

activation and attack of self-antigen (8). The primary pathology of the condition is a gradual degradation of the axon and the myelin sheath brought on by autoimmunity (10) (11). This axonal loss has many consequences for the individual, including irreversible neurological disability, loss of memory, speech disability, and tremors (10) (12). Genetically, MS has been linked mostly to chromosome 6p21, or HLA-DRB1*1501, which has consistently been found in studies across populations (13) (14) (15). There has also been new work done that shows that there may also be influence from chromosome 13q31.3 based on a genome-wide scan of over 500,000 SNPs (16). Genetically, the concordance rate between monozygotic twins is about 25-30%, while the rate between dizygotic twins is about 3-5% (15) (17) suggesting a significant genetic influence on the disease phenotype.

As far as environmental causes are concerned, one primary focus of research has been the role of viruses. For example, the Epstein Barr Virus have been implicated in MS progression (18). Patients that have MS have been found to have high numbers of EBV antibodies in their blood (9). Depending on the time in one's life course, specific factors, such as smoking and Vitamin D intake, may have more an impact on other factors in MS progression (18) (19). Demographically, MS is more likely to affect those of Caucasian descent(20) (21). Other studies have shown that MS incidence in minority population may be underestimated due to factors such as cultural and socio-economic barrier for access to healthcare, as well as a long-standing problem with underrepresentation in clinical trials in general (20) (21).

Diagnosis and clinical course

In 1965, George A. Schumacher proposed the first criteria for MS diagnosis (22). Patients were diagnosed clinically as to having "clinically definable, probable, or possible" MS based on how

many of the six points on the measures were proven to be true (22). The six points for the Schumacher criteria were:

1. Age of onset between 10 and 50 years
2. Objective neurological signs present on examination
3. Neurological symptoms and signs indicative of CNS white matter disease
4. Dissemination in time: two or more attacks separated by a month or progression in symptoms for at least six months
5. Distribution in space: two or more noncontiguous anatomical areas
6. No alternative clinical explanation

The criteria for diagnosing MS has changed over time due to the advent of new technology that can detect anatomical changes in the CNS (22). Poser's criteria modified Schumacher's measures by incorporating paraclinical evidence found through evoked potentials or neuroimaging (22). W.I. McDonald published the most current standards in 2000, which has undergone two revisions since then, with the recent one in 2010 (22) (23). The McDonald criteria sought to get rid of the "probable" diagnosis and incorporate the use of MRI, cerebrospinal fluid (CSF) evaluation, and evoked potentials (23). Establishment of the McDonald Criteria has allowed for a higher diagnostic rate than there was previously (23). Common symptoms of MS include vertigo, mood disorder, pain, sensory disturbance, and fatigue (24). Clinically isolated syndrome (CIS) is a group of symptoms that are typically present at the onset of MS and include optic neuritis, limb weakness, and paresthesia (25). CIS usually lasts for 24 hours or longer and is the first sign of MS caused by neuroinflammation (26). CIS is clinically diagnosed and evaluated (27). If the MRI doesn't show definitive changes in brain

structure, then studies such as assessing the CSF for IgG infiltration and evoked potentials are used (27). MS maybe confused with neuromyelitis optica (NMO), an inflammatory disease that results in visual loss, and acute disseminated encephalomyelitis (ADEM) a form of neurodegeneration that is present in children,based on similarities in clinical presentation (26). Therefore, the Wingerchuk criteria were created for NMO and the magnetic resonance imaging in MS (MAGNIMS)criteria was created for ADEM (26).

MS has four unique clinical progressions: Relapsing-Remitting MS (RRMS), Primary Progressive MS (PPMS), Secondary Progressive MS (SPMS), and Progressive Relapsing MS (PRMS) (28) (29) (Figure 1). RRMS is the most common type, which presents in 85% of MS patients. RRMS is characterized by periods where the disease symptoms occur for a brief period before relapsing for a specified period until the next relapse. PPMS has a course of gradual deterioration and occurs in about 10-15% of MS patients (30). SPMS patients have episodes of symptoms initially, but then the symptoms gradually progress (30). The last type, PRMS, is found very rarely in the population and is characterized by a slow progression of the disease over time with occasional relapses (30). Presentation of MS can be related to age, like those who develop the disease at age 60 or above have a higher chance of developing a more progressive

form (PRMS, PPMS, SPMS) (31).

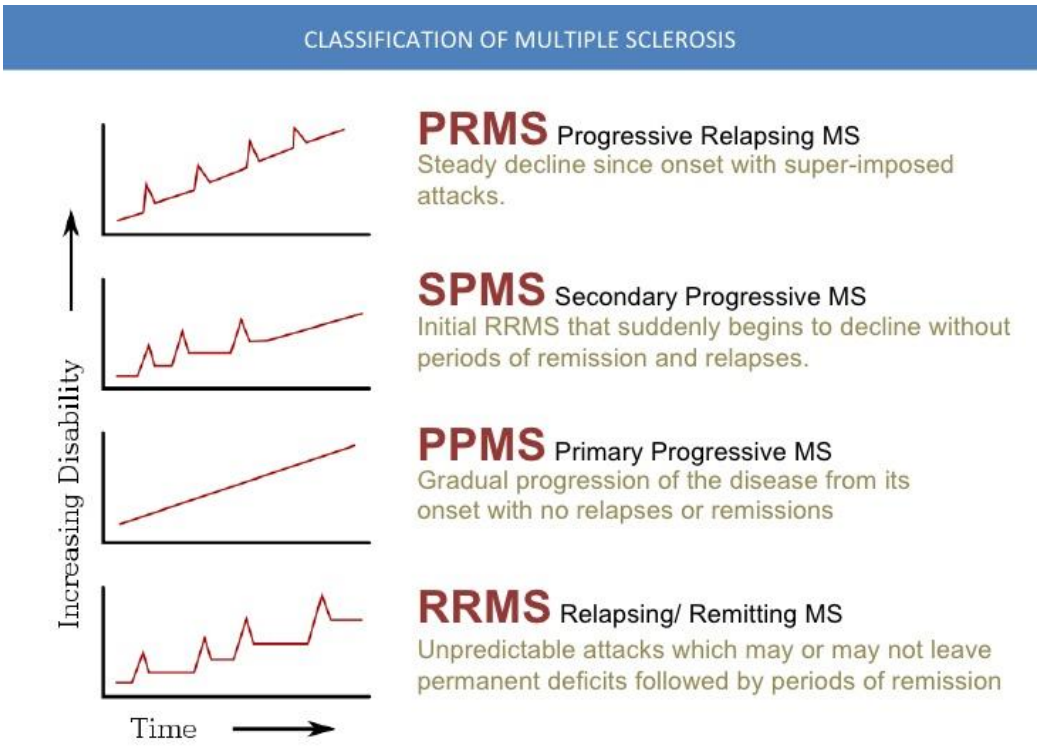

Figure 1: The four different clinical progressions of MS (29)

Imaging

As was previously stated, MS results in demyelination of axons through inflammation (10). The used of imaging has informed researchers about MS pathology and effects. Magnetic resonance imaging (MRI) has played a significant role because of its ability to detect lesions that disseminate in space and time (22) (32). MRI is also useful because it is very responsive to changes in lesions in MS patients (32). It uses protons to assess lesion damage, normal-appearing white matter damage (NAWM) damage, and gray matter damage (32). However, conventional MRI has limitations. Clinical assessment and MRI measures are not always related (32). Another limitation is the lack of ability to identify substrates in individual lesions (32). For

example, inflammation, demyelination, and remyelination all appear similarly on MRI dual-echo images (32). Therefore, it is harder to assess tissue damage. Modifications such as Magnetization Transfer (MT) MRI, diffusion-weighted MRI, and proton MR spectroscopy have been used to find lesions that MRI could not detect (32). MT MRI uses a signal MT ratio (MTR) between free moving protons and protons which are restricted in movement to detect for axonal injury (32). Diffusion-weighted MRI uses the difference in diffusion rates between biological tissues and of water to calculate the apparent diffusion coefficient (ADC) (32). Higher ADC numbers can signify damage (32). Proton MR spectrometry uses decreases in N-Acetyl group levels as a signifier of demyelination (32).

Two other imaging techniques to detect anatomical changes are spectral-domain optical coherence tomography (SD-OCT), which uses head scanning to develop a thickness map of retinal eye tissue, and microperimetry (MP), a technique that produces a spectral map that can determine changes in retinal thickness (33). Optic neuritis (ON) is the first sign of MS in a fifth of MS patients (33). One study found that the volumes of the ganglion cell complex (GCC), retinal nerve fiber layer (RNFL) thickness and macular volume of the retinal ganglion cells (RGC) were reduced in MS patients as compared to healthy control patients (33). The study also a correlation between GCC volume and RNFL thicknes, showing that the ON can affect similar parts in a similar manner (33).

Pathology and pathophysiology

Autoimmunity and inflammation

MS is a neurodegenerative disease caused by an autoimmune response. The activation or triggers for this immune response are not well understood, but there is considerable data on the

significant parts of the autoimmune attack. MS has been long thought to be a CD4+-initiated autoimmune disease, with myelin-specific T-cells causing early demyelination that leads to axonal damage and neurological disability (34). The main T-cells involved in the MS phenotype are T_H1 and T_H17 (8) (34). T_H1 cells produce cytokines such as IFN-γ and TNF-α, which result in a pro-neurodegenerative immune response (35). T_H17 cells have the best ability to cross the blood-brain barrier of all the CD4+ T-cells because of the high expression of cytokine IL-17 (35) Once T_H17 enters the CNS, it can cause damage to neurons through the secretion of granzyme B (34) (35). In the EAE model, there is evidence that T_H1 and T_H17 cells can be isolated in the CNS after crossing the blood-brain barrier (BBB) (35). (8). There have been a number of immunosuppressive therapies that have been or are being developed to reduce T cell proliferation. Mitoxantrone is FDA-approved for immunosuppression (8). It works by decreasing the number of active T-cell lymphocytes (8). IFN-beta works by decreasing T-cell cytokine production (8).

CD8+ T-cells also play a role in MS (8) (35) (36). $CD8^+$ T-cells were found in the active lesions of patients with MS, with high MHC Class I expression (8) (35). Also, the amount of CD8+ T-cells found in the lesions correlated with the amount of axonal damage (36). CD8+ T-cells that are activated by myelin proteins such as MBP or PLP has been shown to cause damage to neurons (36). CD8+ T-cells that are reactive against CNS tissue are interesting because they can escape tolerance induction in the thymus (36). However, CD8+ T-cells have therapeutic opportunities as well, as they can be directed against myelin-specific CD4+ T-cells to kill them (36).

The adaptive immune response in MS is not only limited to T-cells, as plasma cells and their antibodies also play a role in the pathophysiology of MS. From the analysis of patients that have

MS, but there is also evidence of lesions containing autoreactive B-cells and antibodies (8) (37). There is also evidence of oligoclonal bands from those patients that show that a limited number of B-cells is generating the immune response (8) (37) (38). Also found in these lesions are cytokines that function in B-cell development such as B-cell activating factor(BAFF) (38). From the evidence of studying EAE in mice, B-cells are activated by a myelin antigen, such as MOG (8) (37). After activation, B-cells produce antibodies (mainly IgG) that attack axons and myelin (8). There has been evidence that suppressing autoimmune B-cell activation and development can work to alleviate MS symptoms. One therapy being developed against autoimmune B-cells is an anti-CD20 treatment that disrupts immature B-cell growth and proliferation, which reduces the number of immunoglobulins in lesions in MS (37) (38). Patients with MS also present with a high concentration of antibodies in the cerebrospinal fluid, mainly IgG complexes (8). Furthermore, use of immunosuppressants such as IFN-β, mitoxantrone, and glucocorticoids for MS has been shown to reduce inflammation in patients (8), proving to be a valuable way to limit the effects of neuroinflammation.

Other cells in the CNS also play a role in MS pathology. Usually, glial cells such as astrocytes and microglia perform essential functions in the CNS. Astrocytes help regulate the concentration of neurotransmitters and maintain the BBB, while microglia are the phagocytes and antigen presenting cells (APC) of the CNS (39) (40). However, in response to neural insult or injury, glial cells undergo a reactive change that is termed gliosis (41). Astrocytes undergoing gliosis have many damaging effects including antigen presentation, production of nitric oxide (NO), production of pro-inflammatory cytokines, and disruption of axonal metabolism (39). There are less tight junctions maintaining the BBB because of a decrease in tight junction proteins such as claudin 5 (39). Astrocytes also are responsible for forming glial scars that interfere with the

remyelination process (39) (42). Glutamate buffering by astrocytes decreases after injury (42). Their reduced ability to uptake glutamate causes damage to axons as well through the increase in calcium influx by activating NMDA/AMPA receptors (42). Microglia are also more active and increase in proliferation in MS. Microglia mainly damage oligodendrocytes through the production of NO and reactive oxygen species (ROS) (43). Some studies show that microglia may precede the initial T-cell response in MS and are more prominent during the chronic phases of MS (44). Most microglia that are damaging are of the M1 subgroup, while the M2 subset is said to be anti-inflammatory (39). M1 microglia have cytotoxic properties, helping to destroy oligodendrocytes while producing cytokines such as TNF-α. M2 microglia work to promote remyelination of neurons (39) (45).

BBB disruption

The BBB is also disrupted in MS, as a more permeable BBB can often be a sign of MS development (46). Usually, the BBB is composed of endothelial cells and proteins that form tight junctions to keep most solutes out of the CNS (47). It also acts as a regulator for solutes such as oxygen and carbon dioxide to flow down their respective concentration gradients by passive transport (47). Nutrient, drug and protein passage through the BBB is tightly regulated through different channels (47). Also, the BBB protects the CNS from leukocyte infiltration (49). Astrocytes are essential in forming tight junctions between endothelial cells and supplying TGF-β, FGF, and GDNF to these cells as well (48). In MS and other neuroinflammatory diseases, the BBB is disrupted, resulting in increased trafficking of white blood cells and proteins into the CNS. (49). It is not precisely clear what may cause increased BBB permeability, but there are several possible explanations (46) (49). One possibility is that recruitment of lymphocytes by pro-inflammatory cytokines such as TNF, IL-1, and IL-6 to the BBB resulting in increased

permeability of the BBB to white blood cells (49). In addition, NO produced by cells such as microglia can disrupt BBB integrity (49). Another possibility is that cytokines influence the transport of T_{H1} and T_{H17} cells across the BBB (35).T_{H17} cells have been shown to migrate across the BBB due to high expression of IL-17 in that area (35).

Demyelination

Demyelination is understood to be the pathological hallmark of multiple sclerosis (50). In the CNS, myelin is produced by oligodendrocytes and function in saltatory conduction and metabolic buffering (51). In MS, the immune system becomes autoreactive and begins the demyelination process (36). Autoantibodies against myelin proteins such as MBP and PLP and production of NO by activated macrophages actively work to demyelinate the axon (52). The damage from demyelination appears as lesions, of which there are several types. For example, the early active plaques contain macrophages containing myelin debris such as MOG and PLP throughout the lesion and are typically found in patients that are undergoing an acute MS attack, while inactive lesions have macrophages without myelin products and damaged axons (52). Specific demyelinating disorders has standard traits such as the formation of lesions and inflammation. They include Marburg MS, which is very rapid and has large lesion formations in the brain, and Balo concentric sclerosis (BCS), which has a hallmark of concentric lesions (52). In addition to the differences in the types of injuries, there are also differences in how the lesions form (53) (54). Pattern I demyelination is mainly caused by macrophages, while Pattern II involves both macrophages, antibodies, and complement (52) (54). There have also been studies that showed that oligodendrocytes go through apoptosis independent of inflammation, suggesting that there may be some other mechanism for causing demyelination (53). This pattern of demyelination is what is involved in Pattern III, while Pattern IV is rare and deals with non-

apoptotic oligodendrocytes in the peri plaque white matter (PPWM) (52). Demyelinated axons have been shown to be susceptible to degeneration (53), there is also evidence that there is axonal loss happening in inactive lesions as well as active lesions (52). There is also the matter of the differences between demyelination in white matter lesions compared to gray matter lesions, which are less inflammatory but may contribute significantly to the MS phenotype (52) (53). Demyelination in the cerebral cortex is more associated with SPMS and PPMS, while plaques that are considered that have a high number of macrophages in the lesion are more associated with the acute phase of MS (55).

Remyelination is the process where axons are re-covered in myelin following demyelination (56). In MS, there is a process of remyelination where oligodendrocyte progenitor cells (OPCs) remyelinate axons through maturation into oligodendrocytes (56). Specific factors such as Notch signaling, LINGO-1 expression, and PSA-NCAM expression influence the remyelination process (56). With acute lesions, it is possible to have substantial remyelination of exposed axons, although the myelin sheaths will be thinner (56). Microglia also help with the remyelination process by producing cytokines to help with OPC differentiation (40). With chronic lesions, it is highly possible for remyelination to fail because the environment will be less conducive for oligodendrocytes to produce myelin after autoinflammation (52) (56) (57). Remyelination in the later stages is mostly confined to the outer edge of the lesion (52) (56) (57). Astrocytes also interfere with remyelination due to glial scarring that happens after injury (42).

Axonal injury

The result of demyelination and autoimmune attack in the CNS is the gradual loss of axons (58) (59). Axonal density loss during MS is estimated to be around 20% and can affect any part of the CNS (58). Also, the reduction of spinal cord cross-sectional area is determined to be about 25-

37% due to that axonal loss (58). Axonal density loss varies from person to person but gradually increases as the disease progresses (58). The damage from axonal injury can lead to permanent disability, with patients developing fatigue, memory loss, and cognitive impairment (60) (61). The damage to axons results in impaired transport of proteins and organelles, as well as swellings that develop as a result (61). While axon loss is correlated to auto-inflammatory activity, evidence for any direct attack on the axons themselves has been less than sufficient (62). One way that axons can be damaged is through glutamate excitotoxicity that leads to sodium and calcium to accumulate inside of the axon (63). Calcium is of interest because of its ability to activate calpains, which degrade the cytoskeleton of axons (52) (60) (63). Increased calcium buildup has also been studied for its effect on mitochondrial dysfunction. As was discussed previously, demyelination is another factor in axonal loss. With demyelination leading to a redistribution of ion channels leading to metabolic dysfunction in the axon (53). There is also evidence that axonal injury is independent of demyelination. For example, there has been evidence of axonal loss in mice that that had cortical demyelination later in the disease course (61). Also, gray matter lesions experience axonal loss in areas that aren't being actively demyelinated (61).

One of the ways that axonal damage can be identified is by using a marker such as beta amyloid precursor protein (β-APP or Beta-APP). β-APP is highly expressed in neurons (axon, dendrites, and the soma), as well as in vesicles (64). β-APP is transported through the axon using fast anterograde transport by associating with kinesin (64) (65). In autoimmune diseases such as MS, there is a higher expression of APP in neurons affected by MS compared to healthy tissue, and that expression seems to be independent of demyelination (58).

Another way to assess axonal damage is through the expression of non-phosphorylated neurofilament H. SMI-32 is a monoclonal antibody that binds to non-phosphorylated neurofilament H, which can help signify axonal damage. Neurofilament H is the heavy subunit of the neurofilaments, along with neurofilament L (light) and neurofilament M (medium) (67). Neurofilament H is usually phosphorylated at the head domain of the neurofilament, and at the lysine-serine-protein (KSP) motif in the tail domain (66) by MAPKs and dephosphorylated by protein phosphatases such as PP2A (66). Phosphorylation can help to manage subunit interaction and resistance to cleavage (66). When the axon is demyelinated, there is an increase of non-phosphorylated neurofilament H expression (62). Also, there has been evidence that axonal transection leads to a rise in free Neurofilament L and Neurofilament H in the CNS (67).

Wallerian degeneration

Wallerian degeneration is the process of the axons, after injury or disruption of transport, of gradual axonal loss (68). It used to be thought of a process that was passive at first, but test with transgenic mice that have the Wallerian degeneration slow protein (*Wld*^{s}) have led researchers to believe that is a destruction program than causes that axon to break down(69). Similar "dying-back" forms of axonal degeneration happen in other neuronal disorders such as Alzheimer's (69). Wallerian degeneration has been a focus of research for its ability to be delayed, with the possibly of retaining axonal function.

With Wallerian degeneration, there is a latent period (from 4-6 hours in vitro, up to 36 hours *en vivo*) where active fragmentation of the axon does not occur (68). During that latent period, the axon can be protected from irreversible loss by safeguarding its NAD levels (68). There was a study that showed that a rapid increase in NMN, a precursor to NAD, can trigger Wallerian degeneration (70). Wallerian degeneration has been shown to be tied to NAD metabolism inside

the axon, where the rapid loss of NAD interferes with processes such as glycolysis in the axon (68). During the latent period, the NMNAT isoform in the axon (NMNAT2) that would usually work to replenish NAD by combining ATP and NMN to produce NAD is rapidly depleted after injury (68) (71). The *Wld*^{s} protein has an NMNAT domain (NMNAT1) near the N-terminus that has the same functionality as a regular NMNAT protein, signifying that *Wld*^{s} has a similar neuroprotective function (68). After this latent period, the axon continues with rapid demyelination and axonal degeneration (68). The activity of *Wld*^{s} after axotomy can delay the axonal degradation process by 2-3 weeks (68). The *Wld*^{s} protein has an N16 moiety and a Ube4b protein as well, although there is uncertainty about what role each of those play in axon protection (71).

Depending on where the injury occurs, Wallerian degeneration can be beneficial or harmful. In the peripheral nervous system, Schwann cells work right after neuronal damage to remove myelin debris so that the axons can regenerate (72). The Schwann cells also produce laminin so that the axons can be remyelinated and neurotrophic facts such as NGF are also secreted (72). Also, an inflammatory cascade is produced by activated macrophages to clear the myelin (72). The cascade produces pro-inflammatory cytokines and chemokines soon after injury (TNF-α, IL-β) from the Schwann cells and macrophages then produces pro-inflammatory cytokines such as IL-6 from the macrophages to help promote re-growth of neurons (72).

In the CNS, there is evidence that the Wallerian degeneration is more harmful to long term axonal health (72). As opposed to the PNS, the CNS is an immune privileged site, usually protected from the inflammation generally by the BBB that could help clear myelin debris (72). At the same time, the microglia that are activated in the CNS are pro-inflammatory (M1) cause

damage by producing reactive oxygen species (ROS) that demyelinate and damage axons (40) (72).

SARM1

SARM1 is a member of the MyD88 family of TLR adaptors (MyD88, TRIF, TRAM, and Mal) (73). It is also known as MyD88-5 (68) (70) (74). The gene is located on chromosome 17q11 in humans and encodes 690 amino acids (75). The SARM1 protein is highly expressed in neural tissue and is associated with the outer mitochondrial membrane (68). The protein is highly conserved among species such as zebrafish (*Danio rerio)*, horseshoe crab (*Limulidae*), and nematodes (*C. Elegans*) (73). Cluster analysis between Human, *Drosophila Melanogaster*, and *C. Elegans* show that the HEAT/Armadillo repeats in the SAM domain are conserved (75). One of the earliest model organisms for SARM1 testing was *Drosophila Melanogaster*, with the fruit fly homolog *dSarm* shown to promote axonal degeneration (76). SARM1 function has also been studied in mice (*Mus Musculus*) in various contexts such as axonal injury and kainic acid (KA) expression(68) (76). Kainic acid is used to induce excitotoxicity in RGC's, thereby leading to axonal destruction (76) SARM1 depletion resulted in preserving retinal nerve structure by attenuating for KA (76). Figure 2 shows the domains of the protein (68).

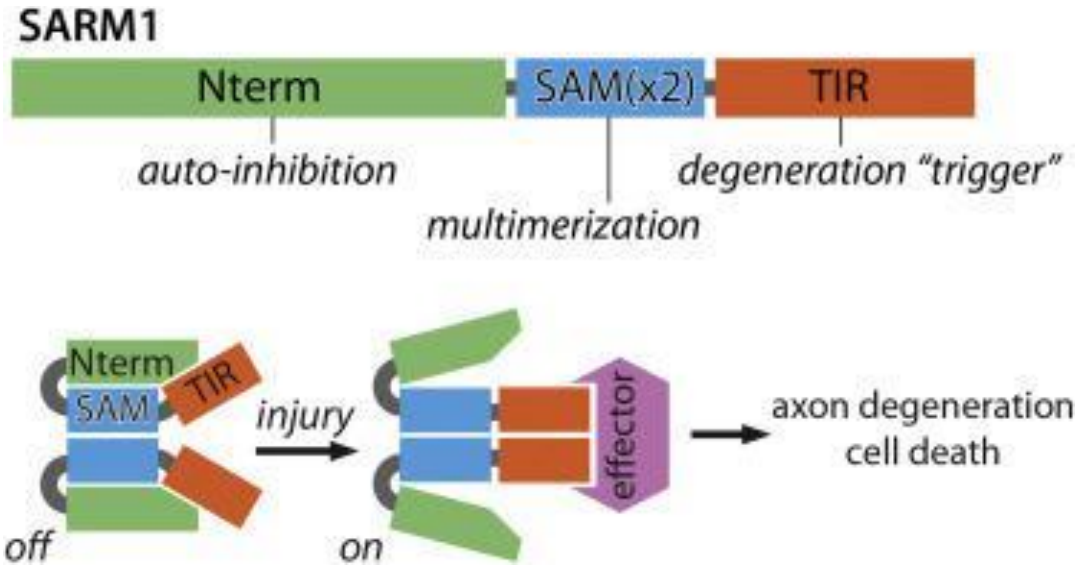

Figure 2: Theoretical figure and activation for SARM1. SARM1 is usually autoinhibited by the N-terminal domain. After injury, SAM domains multimerize and the TIR domains are activated. The multimerized TIR domains go out to activate effectors that deplete NAD+ (68).

SARM1 in inflammation

SARM1 has been studied for the different roles it plays in inflammation. Depending on the context, it can either activate or deactivate inflammation. Unlike the other members of the MyD88 family, SARM1 does not activate the NF-κB pathway but enables the MAPK pathway through its TIR domain activating MKK4 through ASK, which goes on to activate JNK and p38 and result in expression of genes involved in the immune response (77) (78). Blocking inflammation by deleting MKK4 or using AKT to antagonize MKK4 has neuroprotective effects (68). JNK also works to cause axonal degeneration by targeting stathim 2 (SGC10), a cytoskeletal protein, for degradation (68). That results in eventual degeneration of the whole axon (68). Figure 3 shows how SARM1 upregulates JNK and p38 expression while suppressing TRIF dependent signaling that relies on stimulation of TLR 3/4 inside a CD8+ T-cell (73) (77).

SARM1 also helps stimulate TLR7/9 mediated apoptosis in neurons though localization to the mitochondria and subsequent mitochondrial accumulation inside neurons (79). In a study by Szretter et. Al, mice were infected with West Nile virus (WNV)(80). SARM1 deficiency worked to decrease TNF-α production in the CNS, leading to higher mortality in mice infected by WNV (80). SARM1 deficient mice also had lower microglia activation (80) (81).

SARM1 can also work to decrease cytokine production (77) (81). SARM1 in the neuron can work to decrease cytokine production by blocking the TRIF-dependent pathway and instead activate the MKK4 pathway that results in the activation of Bax, an effector of apoptosis (77). SARM1 knockout mice were shown to have higher levels of IL-6 and IFN-Beta in embryonic neurons (81). In adult neurons, SARM1 knockout mice have higher levels of IL-1-beta and IL-12b (cytokines of the NF- κB pathway) (81).

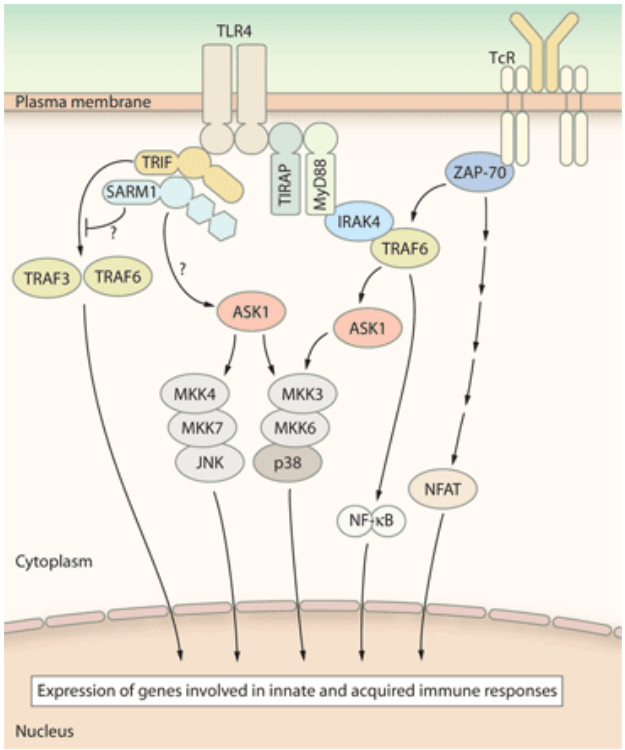

Figure 3: SARM1 activates the JNK/p38 pathway in CD8+ T-Cell. SARM1 activates ASK1, which phosphorylates MKK4 in the MAPK pathway. JNK and p38 are activated and go to the nucleus to activate cytokine production. SARM1 also inhibits the TRIF-dependent pathway from TLR4 signaling (77).

SARM1 in axonal degeneration

SARM1 causes axonal damage by NAD+ cleavage (68) (82). The SARM1 protein is usually auto-inhibited by its N-terminal domain, but following axonal injury, the SAM domains allow for dimerization of SARM1, leading to activation of its effector function that results in cleavage of NAD (68) (82). Lower NAD+ levels can result in axonal metabolic dysfunction, resulting in an influx of Ca^{2+} and subsequent activation of calpain (52) (60) (63) (68). Research done in the nematode found that cleavage of NAD required dimerization of the TIR domains in *C. elegans* (TIR-1), although the deletion of NAD+ was not as robust as in human SARM1 (82). Neurons in mice that have SARM1 deleted has ATP and NAD levels that remain at normal levels, and as a result have axons that can survive longer, like the effects of *Wld*^{s} (82). Also, axons have an endogenous NMNAT (NMNAT2) that can inhibit SARM1 by synthesizing NAD+ (68). Lower NAD+ levels in the axon because of NMNAT2 loss or inactivation has been theorized to activate SARM1 (68) (82). Another way that SARM1 is activated is explained by the NMN hypothesis. According to the hypothesis, higher NMN levels are responsible for triggering SARM1 (68). NMNAT2 works to consume NMN and ATP and make NAD+, thus preventing activation (68). Figure 4 shows how SARM1 functions to trigger axonal degeneration (68).

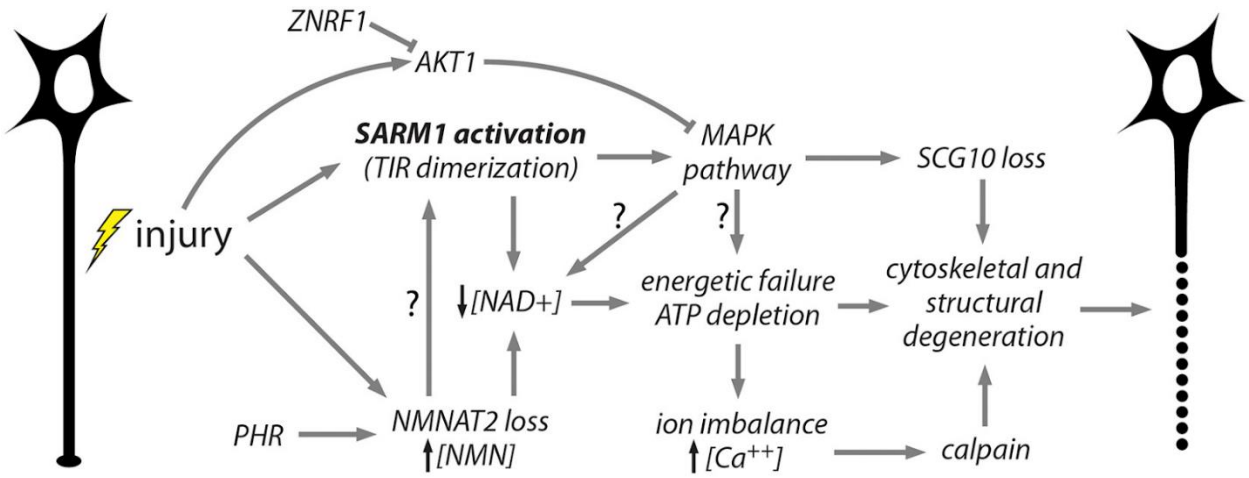

Figure 4: SARM1 axonal degeneration pathway. As SARM1 is activated, TIR dimerization results in NAD+ depletion and MAPK activation. Eventually, ATP is depleted, and the axon begins to break down.NMNAT2 loss also results in SARM1 activation. (68)

Experimental allergic encephalomyelitis

Experimental allergic encephalomyelitis is an animal model of MS that has been used to understand possible causes and effects of the disease (83). It has also been used to test treatments for MS, such as using IFN-β or glucocorticoids for immunosuppression (83). The disease was first studied in primates but has since included other animals such as mice and guinea pigs (53) (83). Unlike MS, the animal must be inoculated with a myelin antigen (usually MBP or MOG_{35-55}) and adjuvant (usually CFA) to produce the EAE phenotype (83). Once the animal has been inoculated, EAE develops as the animal is monitored over several days. There are similarities be between EAE and MS. In EAE and MS, there is increased T-cell infiltration and demyelination, increased adhesion molecule expression, and increased cytokine production (8) (84) (85). There are differences between EAE and MS that are important to note, such as the heterogeneity of disease progression and the heterogeneity of effects across species (8). However, EAE has been

proven to be an excellent way to study the effects of MS. There has been prior research that has used SARM1 expression to research nerve protection in mice and other animals (68). In the mouse, the gene for SARM1 is found on chromosome 11 (86). Inactivation has shown some evidence of axonal protection and lower inflammation. SARM1 silencing in mice was shown to lower axonal degeneration in the retinas (77). SARM1 inactivation leads to preserved NAD+ levels in *Drosophila* flies (82).

Hypothesis

We hypothesize that SARM1 works to cause breakdown of axons by interfering with the local metabolism of the axon after the autoimmune attack and that axons can be rescued by inactivating the protein genetically. Using EAE as a model for MS, we aim to understand how SARM1 inactivation affects axonal degeneration. Preliminary data has shown a modest reduction in clinical EAE score over the first couple of weeks post-induction and a lower clinical score overall.

Specific Aims

S1: Establish EAE pathology

EAE will be induced in several mice using CFA+MOG_{33-55}. Clinical scores will be assessed daily over the course of a six-week period. IHC will be used to determine inflammation (CD3) and axonal health (Beta-APP, SMI-31/32) in healthy and EAE mice.

S2: Assess SARM1's impact on axonal integrity

The specific aim is to examine the effect of SARM1 on axonal degeneration in the context of EAE. End-point PCR and qRT-PCR will be used to assess genotype and gene expression.

Western Blotting and ICH will be used to validate antibodies. YFP expression and Beta-APP expression will be used to measure the amount of axonal degeneration to quantify SARM1's impact of axonal damage.

METHODS

Mice

Sarm1 KO (B6.129X1-*Sarm1*^{tm1Aidi}/J) mating pairs were obtained from Jackson Laboratories (Bar Harbor, ME). A breeding colony of *Sarm1* KO mice was then maintained in-house. A heterozygote mating scheme generated *Sarm1* KO and WT littermates for the EAE experiments. *Thy1-YFP* (B6.Cg-Tg(Thy1-YFP)HJrs/J) mating pairs were a kind gift from John Povlishock. The *Thy1-YFP* mice express yellow fluorescent protein (YFP) at high levels in motor and sensory neurons, as well as subsets of central neurons. Axons are brightly fluorescent all the way to the terminals. A breeding colony of *Thy1-YFP* mice was maintained in-house. To generate *Sarm1* KO mice that express YFP in neurons, we crossed mice hemizygous for the *Thy1-YFP* transgene and Sarm1 KO mice to yield *Thy1-YFP*/*Sarm1*$^{+/-}$ mice. *Thy1-YFP*/Sarm1$^{+/-}$ breeding pairs were maintained to generate Thy1-YFP/Sarm1$^{-/-}$ and Thy1-YFP/Sarm1$^{+/+}$ littermates for EAE experiments. All mice were C57BL/6 background.

EAE

EAE was actively induced by injection of myelin oligodendrocyte peptide (MOG_{35-55}) in complete Freund's adjuvant and injection of pertussis toxin. Sham control mice were injected with complete Freund's adjuvant without MOG_{35-55}. Clinical severity was scored according to a standard 5-point scale: 0 = normal, 1 = limp tail or loss of righting reflex, 2 = limp tail and loss of righting reflex, 3 = partial hind limb weakness, 4 = hind limb paralysis, 5 = moribund or

death. The cumulative clinical score was calculated as the sum of daily clinical scores over the course of observation.

DNA Purification

DNA was purified from tissue using the DNeasy Kit (Qiagen) according to manufacturer's protocol. Tail clippings were digested in 180 µL of buffer ATL and 20 µL of proteinase K and kept overnight at 56℃. 200 µL of Buffer AL and 200 µL of 100% ethanol was added to tail tissue. The product was then vortexed. The mixture was then pipetted into a DNeasy spin column in a two mL collection tube. The mixture was centrifuged at 6000 x g for 1 min at room temperature. The spin column was placed in a new 2 mL collection tube. 500 µL of Buffer AW1 was then added. The product was centrifuged at 8000 rpm for 1 minute at room temperature. The spin column was then placed in a new 2 mL collection tube. 500 µL of Buffer AW2 was added. The product was centrifuged at 14,000 rpm for 2 mins at room temperature. The spin column was then placed in a 1.7 mL microcentrifuge tube. 200 µL of Buffer AE was added to the mixture to elute the DNA. The product was then incubated for 1 min at room temperature. The mixture was centrifuged at 8000 rpm for 1 min at room temperature. Concentrations were measured spectrophotometrically on a BioTek plate reader.

Sarm1 genotyping

Sarm1 genotyping was performed by PCR. The reaction mixture comprised of DNA, PCR mastermix (Amplitaq Gold 360 MasterMix, Applied Biosystems) and primers. *Sarm1* knockout forward and reverse primers were CTT GGG TGG AGA GGC TAT TC and AGG TGA GAT GAC AGG AGA TC, respectively. *Sarm1* wild type forward and reverse primers were GGG AGA GCC TTC CTC ATA CC and TAA GGA TGA ACA GGG CCA AG, respectively. Each PCR reaction well contained 12.5 µL of mastermix, 2.5 µL of forward and reverse primers and

10 µL of DNA sample (50 ng). A non-template control well was included for each assay. The Venti Thermal Cycler was set with the Amplitaq Gold 360 run protocol for a 25 μL reaction: The samples were heated for 10 minutes at 95℃. Then, they went through 40 cycles of initial denaturation at 95℃ for 30 second, primer annealing at 60℃ for 30 seconds, and extension at 72℃a at 60 kb/second. The final extension was for 7 minutes at 72℃. The samples were cooled at 4℃ after the final extension was complete.

The PCR product was analyzed by gel electrophoresis. 50 mL of 2% agarose with 5 µL of Gel Red was poured into a beaker, then into a DNA Plus electrophoresis well and allowed to solidify with 2 combs placed inside the gel. 1x TBE buffer (0.089 M Tris Base, 0.089 M Boric Acid, 0.002 M Disodium EDTA·2H_2O) filled the well so that the gel was covered. 5 µL of ddH_2O was mixed with 2 µL of Blue/Orange 6x loading dye on parafilm. 5 µL of PCR product or the NTC was mixed with ddH_2O and 6x loading dye and loaded into the gel. The gel ran at 80 V for about an hour. The gel image was taken with an Aplegen Imager.

RNA Purification

RNA was purified from mouse tissue. Following euthanasia, brain, liver, kidney, spleen, and testis were harvested from mice and placed in a 1.7 mL microcentrifuge tube with 350 µL of RNAlater (Qiagen) was added to preserve RNA for later use. Tissues were lysed using a TissueLyser LT. Briefly, stainless steel beads were added to each tube. 1 mL of QIAzol reagent was then added to each tube. Tissues were lysed for 5 min at 50 Hz and then left to stand for 3-5 minutes. The stainless-steel beads were then discarded using a small spatula. Chloroform (200 µL) was added to each tissue sample inside the fume hood. The tissues were then centrifuged at 12,000 x g for 15 minutes at 4℃. After centrifugation, the mixture was separated into an aqueous top layer, a white interphase layer, and a pink organic layer. About 400 µL of the aqueous layer

was transferred to a 1.5 mL RNAse free tube containing. 400 µL of 100% ethanol. The resulting mixture was then transferred to RNeasy mini spin columns (Qiagen) for RNA purification according to manufacturer's protocol. The columns were placed on a vacuum manifold. The columns were washed with 700 µL of buffer RW1, 500 µL of buffer RPE, and 500 µL of buffer RPE, sequentially, using the vacuum after each addition. After the washing, the columns were placed in 2 mL collection tubes. The columns were then dried by centrifugation at full speed (21,100 x g) for 1 minute. The columns were then placed in 1.5 mL collection tubes. 50 µL of RNAse-free water was then added to the columns to elute the RNA. The columns were then centrifuged at 8000 x g for 1 min. RNA concentration was measured spectrophotometrically using a BioTek plate reader. The RNA samples were stored in a -80℃ freezer until later use.

Quantitative reverse transcriptase (qRT)-PCR

Sarm1 RNA expression was measured by real-time RT-PCR. TaqMan mastermix, *Actb* primer/probe, *Sarm1* primer/probe mix (Mm_001308995_m1 Thermo Scientific), which spans *Sarm1* gene exons 1 and 2, *Sarm1* primer/probe mix (Mm_00555617_m1, Thermo Scientific), which spans *Sarm1* genes exons 7 and 8, and reverse transcriptase were thawed in PCR/UV box. Wells were planned out for each RNA sample so that 10 µL of mastermix, 1 µL of each primer/probe, 0.5 µL of reverse transcriptase and 8.5 µL of diluted sample were added to each well. A non-template control (NTC) of ddH_2O was also used for the wells. A working mixture of mastermix and primers was made and aliquoted into wells. Wells were taken into biosafety cabinet, and RNA was aliquoted into wells. Wells were capped and centrifuged at 1000 rpm for 2 min. The samples were placed into the StepOnePlus Real-Time PCR machine. 2-step singleplex RT-PCR was run to convert RNA into cDNA and to amplify cDNA expression: WT Spleen was set as the reference sample, and *Actb* was used as the endogenous control for the comparative C_T

experiment. Samples were heated from 25℃ to 95℃ for 10 minutes in the holding stage and then ran through 40 cooling and heating cycles between 60℃ and 95℃ for 1 minute each. Fluorescence was measured using the StepOnePlus machine.

Western Blotting

WT brain, WT liver, *Sarm1* KO brain, and *Sarm1* KO liver protein samples were diluted to 6 mg/mL using cold lysis buffer (RIPA buffer, ThermoScientific) and 1x Protease Inhibitor Cocktail). The samples were further diluted to 3 mg/mL by 100µL working Lammeil Buffer (950 µL of 2x Lammeil Buffer and 50 µL of 2-mercaptoethanol). The samples were resolved in a Mini Protean Precast gel (10-well, 30 µL per well) at 200 V for 35 minutes. The was prepared for transfer of the protein. The product was then transferred to a nitrocellulose membrane through the Bio-Rad Trans-Blot Turbo Transfer System with 1x turbo blot transfer buffer (50 µL 5x Turbo Blot Transfer Buffer (BioRad), 50 µL of 200 proof ethanol, and 150 µL of deionized water). The membrane was then agitated with Ponceau S for 10 minutes, washed with deionized water, then imaged with an Aplergen imager. Then the membrane was washed with PBS-Tween 3 times for 5 minutes each. The membrane was then blocked with PBS-Tween-5% milk for 30 minutes. The membrane was then stained with the diluted primary antibody (Rat Anti-SARM1, Biolegend, 1:1000 in PBS-Tween) and agitated at 4℃ overnight. The membrane was washed with PBS-Tween 3 times for 5 minutes each. The membrane when stained with secondary antibody (CARt-HRP, Santa Cruz, 1:5000 in PBS-Tween) and agitated for 45 minutes at room temperature. The membrane was washed with PBS 3 times for 5 minutes each. Less than 1 mL of Millipore immobilon reagent was applied to the membrane. The membrane was then imaged with an Aplergen imager using the Chemiluminescence setting. The membrane was then stripped and reblotted for Beta-Actin as an endogenous control. Mouse Anti-β Actin, (ThermoScientific,

1:5000 in PBS-Tween) was the primary antibody, while DAM-HRP, (ThermoScientific,1:5000 in PBS-Tween) was the secondary antibody.

Fluorescent Immunohistochemistry

Parts of the mouse CNS were surgically removed from mice and placed in optimal cutting temperature (OCT) cryopreservative and stored at -80°C. 20 µm sections or 10 µm sections (SMI-31/32) and using a Lecia CM 1950 cryostat and placed on positively charged slides. The sections had a PAP border drawn around them after the OCT as trimmed. All sections were rinsed in 1x TBS (Fisher Bioreagents) after sectioning, after primary antibody application, and after secondary antibody application 3 times for 5 minutes each. Blocking buffer (970 µL of TBS, 2 drops of cold skin fish gelatin (EM Sciences #25560) and 30 µL of 10% Triton X-100) was used for blocking.

Primary antibodies stained for Beta-APP (Rabbit Anti-Beta APP, Thermoscientific, 1:400), SARM1 (Rat-Anti SARM1, Biolegend, 1:200), NeuN (Mouse unconjugated Anti-NeuN, Millipore,1:100), SMI-31 (Mouse SMI-31, Calbiochem, Cat No. NE1022, 1:1000), SMI-32 (Mouse SMI-32, Calibiochem, Cat. No. 1023, 1:1000), CD3 (Hamster Anti-CD3, BD Biosciences, 1:100), and CD31 (Rat Anti-CD31, ThermoScientific, 1:50). Sections were placed in a 4°C refrigerator overnight for primary staining (60 minutes for CD3/CD31 at room temperature), and at room temperature for 90 minutes (60 minutes for CD3/CD31) for secondary staining in a closed, moisturized box. Sections were blocked for 15 minutes before primary and secondary staining at room temperature. All sections were stained with either primary antibody or blocking buffer before secondary staining. Secondary antibodies used for this project were Rabbit IgG Alexa Fluor® 594 antibody, Goat Anti-Rat IgG Alexa Fluor® 594, Goat Anti- Mouse IgG Alexa Fluor® 488, and Goat Anti-Hamster IgG Alexa Fluor® 488 (all 1:1000). DAPI

(Vectashield®) was used as a counter-stain before imaging and coverslips were purchased from Corning. Digital images were taken with a Life Technologies ™ imager, then modified using the Fiji program from the NIH (87). Every fifth lumbar cord section was stained for Beta-APP. Every fifth lumbar cord section was mounted for YFP^+ axonal counting. Beta-APP particles and YFP^+ expressing axons were manually counted using Fiji (87).

Antigen Retrieval

Sections were placed in a plastic coplin jar of 40 mL citric acid buffer (pH 6.0). Another plastic coplin jar was filled with 40 mL of ddH_2O. The two coplin jars were both placed in a microwave, and a thermometer was placed in the coplin jar that was filled with deionized water. The sections were microwaved at 525 W with a 45℃-maximum temperature for 7 minutes. The sections were then removed from the microwave and allowed to sit for 5 minutes. The sections were microwaved at 525 W with a 45℃-maximum temperature for 5 minutes and 30 seconds. The sections were then removed from the microwave and allowed to sit for 20 minutes. Afterwards, the slides were then washed rapidly in 1x TBS 3 times.

M.O.M protocol -SMI-31/SMI32 (Neurofilament H)

Sections were fixed in pre-chilled 100 % methanol for 10 minutes at -20℃ after antigen retrieval. A working solution of Vector M.O.M ™ Mouse IgG Blocking reagent (FMK-2201) was prepared by adding 60 µL of the stock solution to 2.5 mL of TBS. A working solution of M.O.M ™ Diluent was prepared by adding 600 µL protein concentrate to 7.5 mL of TBS. The sections were then washed 3 times in TBS for 5 minutes each. Then each of the sections was incubated with Mouse IgG blocking reagent for 1 hour. Then the slides were washed in TBS twice for 2 minutes each. The primary antibodies and were diluted in M.O.M ™ Diluent. Mouse

SMI-31 was applied to an EAE lumbar cord section and a healthy lumbar cord section. Mouse SMI 32 antibody was applied to an EAE and healthy lumbar cord sections. M.O.M ™ Diluent was applied to an EAE section as a control. The slides were incubated overnight in a closed, moisturized box in a 4℃ refrigerator. On the next day, the sections were washed in TBS twice for 2 minutes each. A working solution of M.O.M ™ Biotinylated Anti-Mouse IgG Reagent was prepared by adding 10 µL of stock solution to 2.5 mL of M.O.M ™ Diluent. M.O.M ™ Biotinylated Anti-Mouse IgG Reagent was applied to each section, and the sections were incubated for 10 minutes. The sections were then washed in TBS twice for 2 minutes each. A working solution of Texas Red Avidin DCS was prepared by adding 40 µL of stock solution to 2.5 mL of TBS. Texas Red Avidin DCS was applied to each section and incubated for 5 minutes. The slides were washed in TBS twice for 5 minutes.

YFP$^+$ axonal counting

Axons were manually counted by drawing three vertical lines to contact the axons and then manually counting the axons at the contact points along the longitudinal tracts using Fiji (87). Degrading axons were identified by focal swellings or fragmentation along the axon.

Statistical Analysis- YFP$^+$ and Beta-APP

Mann-Whitney tests were used to compare WT (N = 4) and *Sarm1* KO (N = 3) mouse littermates for YFP$^+$ expressing axons, degrading axons, and Beta-APP particles. The p-value calculator for the test was found on http://astatsa.com/WilcoxonTest/. Statistically significant p-values for this experiment were $p < 0.05$.

RESULTS

Sarm1 *KO mice*

Sarm1 KO mice were genotyped by PCR. Figure 5 shows the *Sarm1* PCR products for the WT, heterozygote and *Sarm1* KO mice. PCR using primers for *Sarm1* and WT alleles resulted in bands near the expected 280 bp and 186 bp, respectively. *Sarm1* KO and WT alleles were both present in heterozygotes.

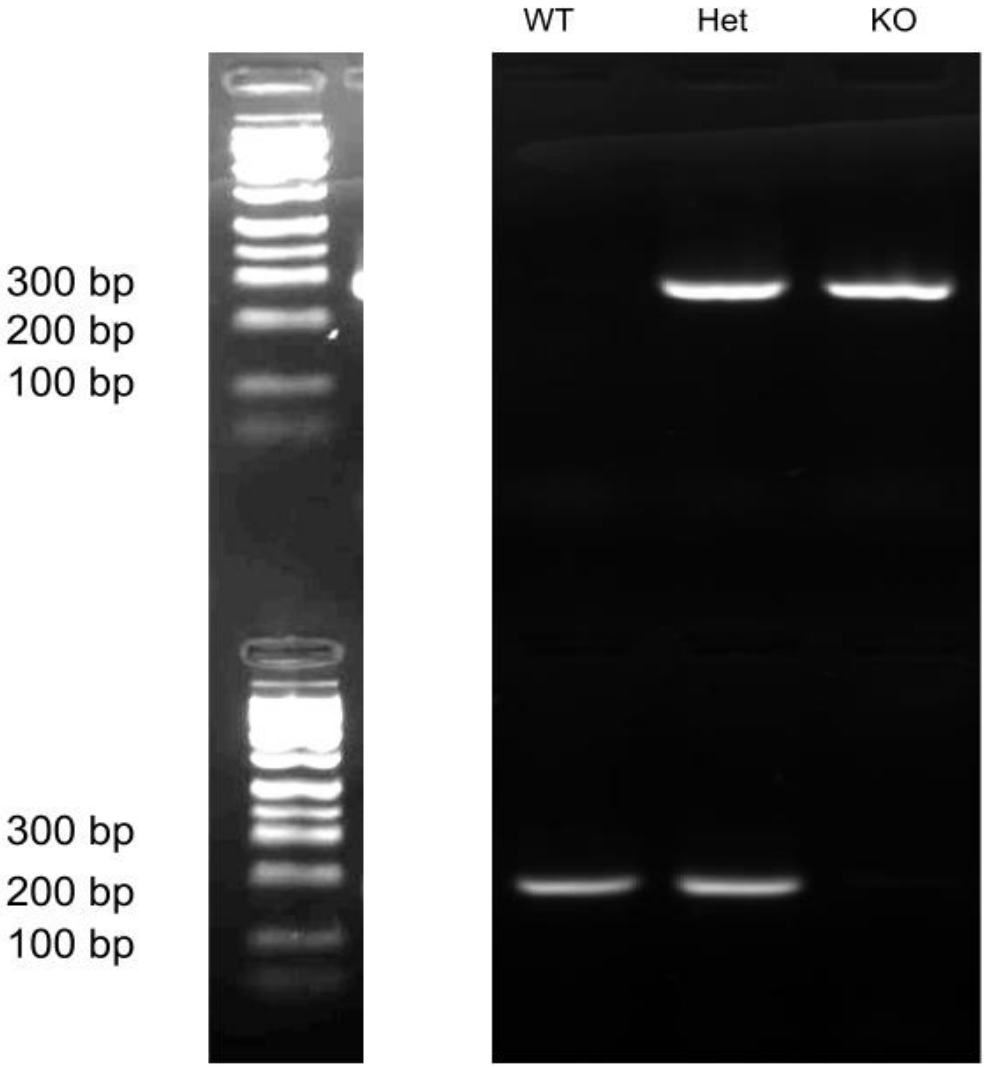

Figure 5. *Sarm1* genotyping by PCR. DNA was isolated from mice tail clippings. End-point PCR was performed using primers targeting *Sarm1* KO and WT alleles. A representative agarose gel electrophoresis is shown with PCR products for mice homozygous for the WT allele (WT),

heterozygote (Het), and homozygous for the *Sarm1* KO allele (KO). DNA ladder denoting size is shown on the left.

Sarm1 mRNA expression

Sarm1 mRNA from brain, kidney, spleen, liver, and testis of WT mice were measured by quantitative reverse transcriptase (RT)-PCR to determine the relative *Sarm1* expression among different tissues. Figure 6 shows *Sarm1* gene expression for each tissue type. *Sarm1* expression was highest in the mouse brain, followed by the testis. *Sarm1* expression was low in the kidney, spleen, and liver (Figure 6).

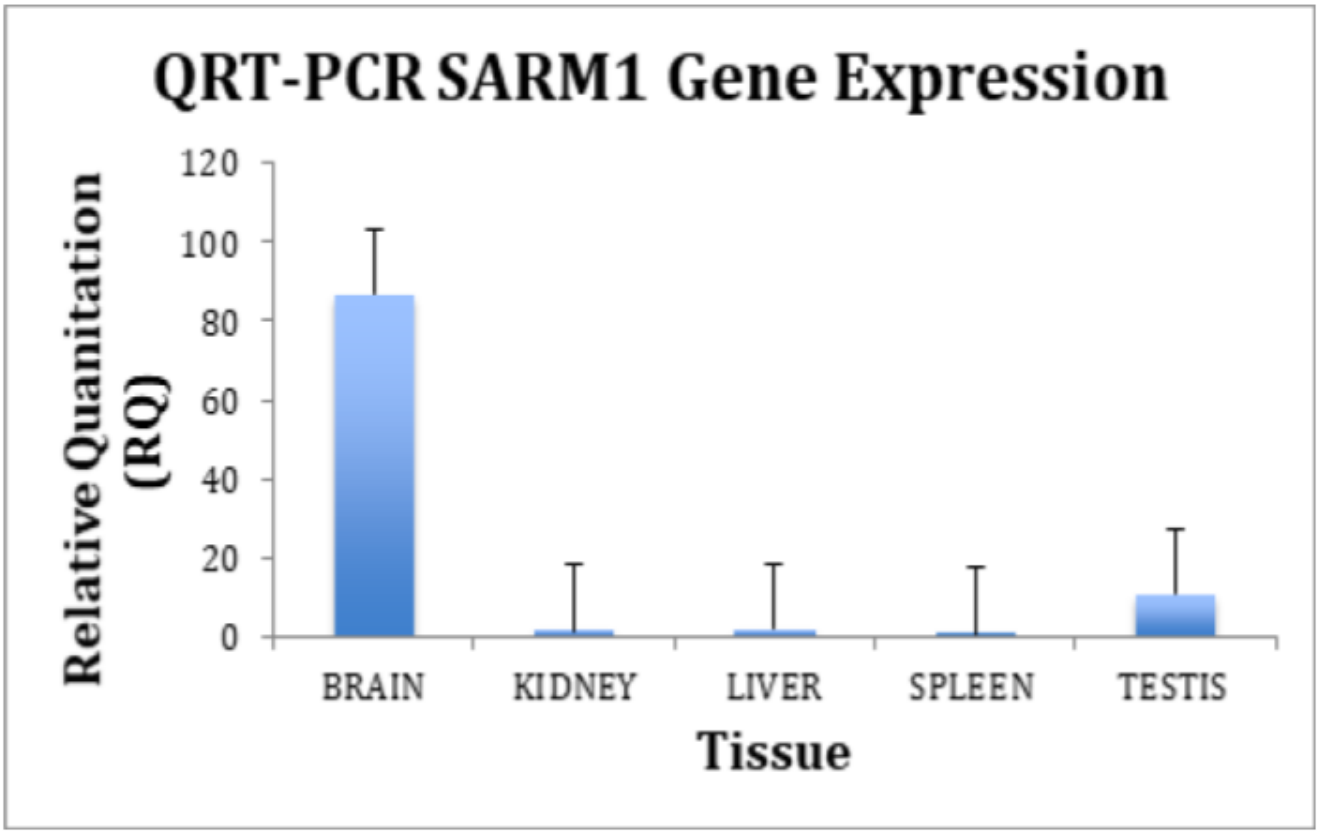

Figure 6: *Sarm1* gene expression in different tissues. Genomic DNA was isolated from various mouse tissue, then quantitative RT-PCR (QRT-PCR) was performed to measure relative *Sarm1*

mRNA expression. Relative quantities (RQ) were calculated using the $\Delta\Delta C_T$ method. *Actb* was used as the endogenous control. Spleen was used as the reference sample. N = 3 for brain, spleen, liver, and kidney; N = 2 for testis. Mean (+S.E.M) shown.

To further characterize how *Sarm1* gene expression is altered in the *Sarm1* KO mice, qRT-PCR was performed using primers directed against either the 5' or the 3' regions of the *Sarm1* transcript. One primer/probe set spanned exons 1 and 2 of the *Sarm1* transcript, and the other spanned exons 7 and 8 of the *Sarm1* transcript. Figure 7 shows the relative *Sarm1* expression in WT and *Sarm1* KO brain using the two *Sarm1* primer/probe sets. As expected, WT brains showed relatively high *Sarm1* mRNA expression with primer/probes spanning either exons 1 and 2 or exons 7 and 8. We detected *Sarm1* mRNA expression in the *Sarm1* KO brain using primer/probes spanning exons 1 and 2, although at a substantially lower level compared with WT. *Sarm1* KO brains showed no mRNA expression when qRT-PCR was performed with primer/probe set spanning exons 7 and 8. These results showed that in the *Sarm1* KO mice, exons 7 and 8 of *Sarm1* gene are not transcribed, indicating that a truncated *Sarm1* mRNA is produced in the *Sarm1* KO mice.

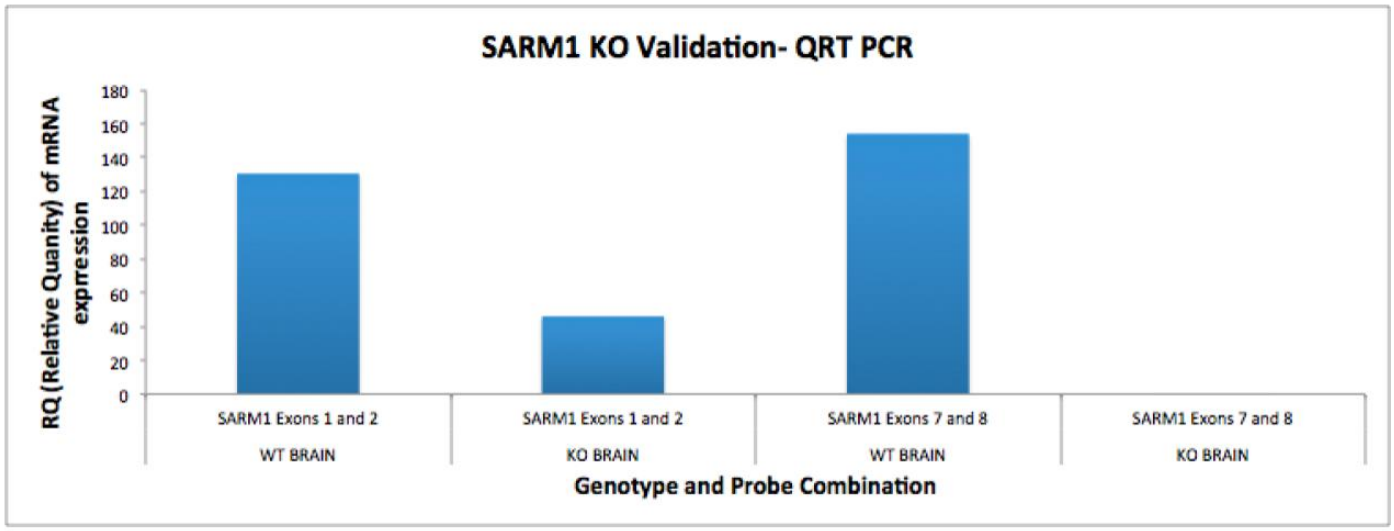

Figure 7. *Sarm1* gene expression in brain tissue based on genotype and probe combinations. mRNA was either amplified with *Sarm1* primer/probe set 1309985 that spans exons 1 and 2 or *Sarm1* primer/probe set 555617 that spans exons 7 & 8. RQ values are shown.

EAE pathology

Initial studies with EAE were aimed at establishing methods to assess pathologic changes associated with EAE by immunohistochemistry. CNS inflammatory infiltrates were detected by CD3 immunohistochemistry. Axonal pathology was identified by APP and SMI-31 and SMI-32 immunohistochemistry. EAE was compared with sham or healthy controls.

CD3 immunohistochemistry

CD3 immunohistochemistry was performed to assess inflammation in EAE mice. Figure 8 shows CD3 immunohistochemistry for EAE and sham control mice. PECAM immunohistochemistry was performed simultaneously to identify blood vessels. There is more CD3 marker staining in

the EAE lumbar cord than in the lumbar cord of the sham control mouse, showing CNS T-cell infiltration in EAE.

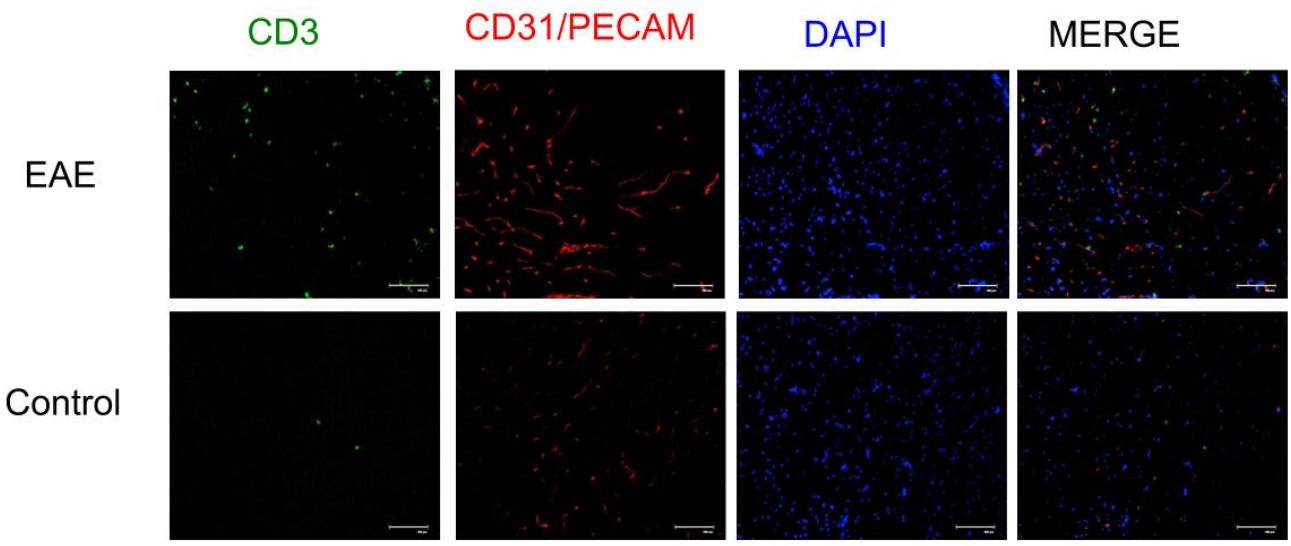

Figure 8. Increased CD3 staining in EAE lumbar cord. CD3, CD31/PECAM, DAPI, and merged images shown. Scale bar = 100μm.

SMI 31/32 immunohistochemistry

Neurofilament H immunohistochemistry was performed using SMI-31 and SMI-32 to assess axonal integrity in EAE mice. Figure 9 shows SMI-31 immunohistochemistry of longitudinal sections of the lumbar cords of EAE and the sham control mice. As Figure 9 show, there is comparable staining, shown in red. Figure 10 shows SMI-32 immunohistochemistry of lumbar cord of the EAE and sham control mice. Comparing the two pictures shows that there is more non-phosphorylated neurofilament-H in the EAE mouse.

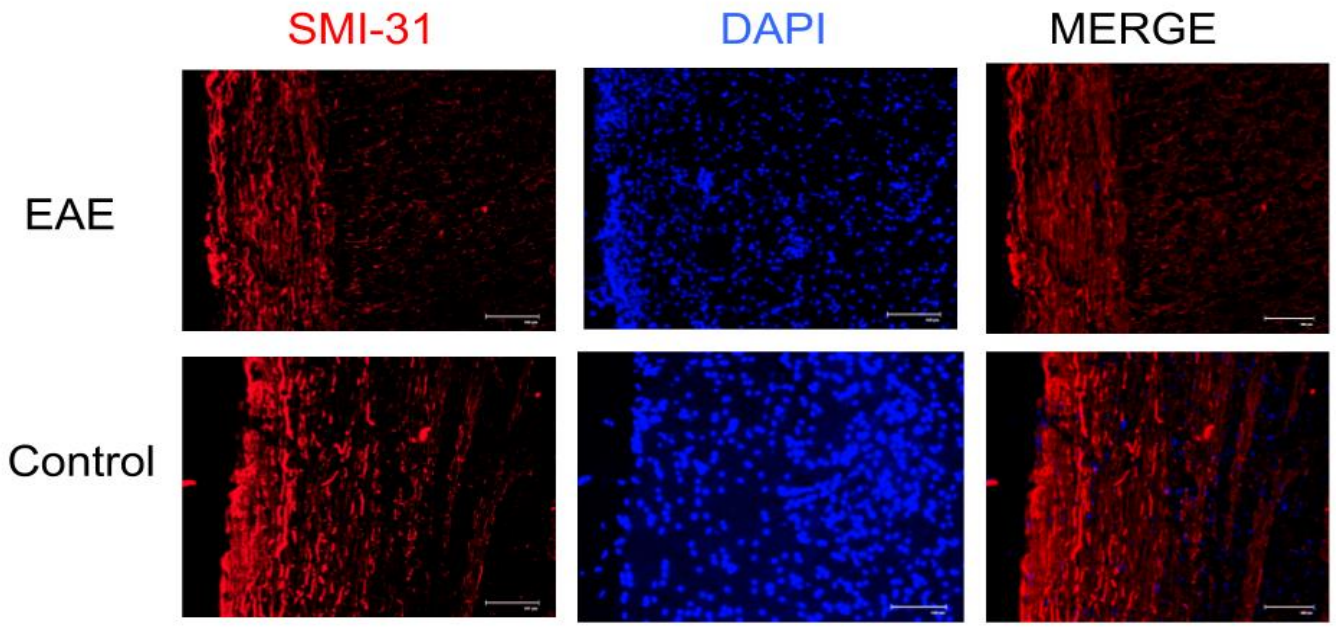

Figure 9: Comparable phosphorylated neurofilament H (SMI-31) staining in EAE and healthy lumbar cords. Representative phosphorylated neurofilament H, DAPI, and merged images are shown. Scale bar = 100μm.

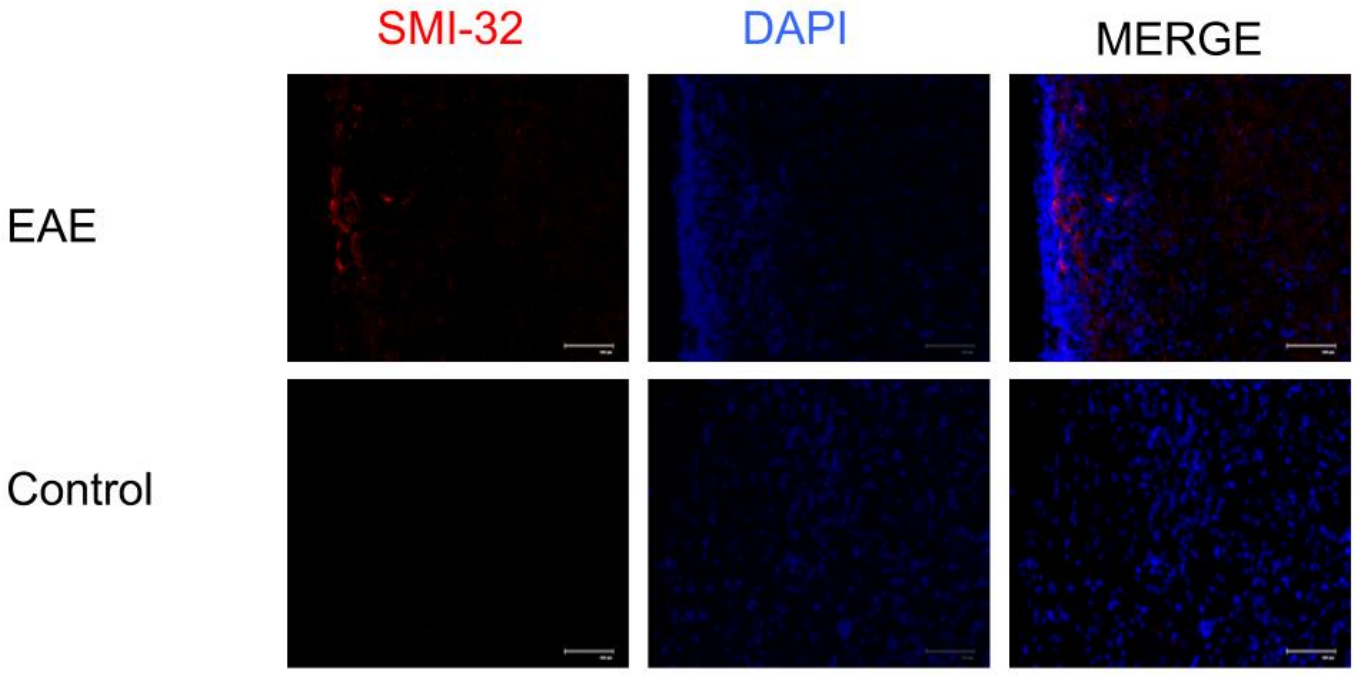

Figure 10: Increased non-phosphorylated neurofilament H (SMI-32) staining in EAE mouse. Lumbar cord sections for EAE and control mice were stained for the axonal marker non-phosphorylated neurofilament-H. Representative non-phosphorylated neurofilament-H, DAPI, and merged images are shown. Scale bar = 100μm.

B-APP immunohistochemistry

Beta-APP immunohistochemistry was utilized to assess axonal damage in EAE mice. Beta-APP, DAPI, and multichannel (+YFP) images (Figure 11) of the longitudinal sections of the lumbar cord of an EAE mouse and a healthy mouse. Comparing the two sets of images shows that there is reduced Beta-APP particles in the EAE lumbar cord than in the healthy lumbar cord.

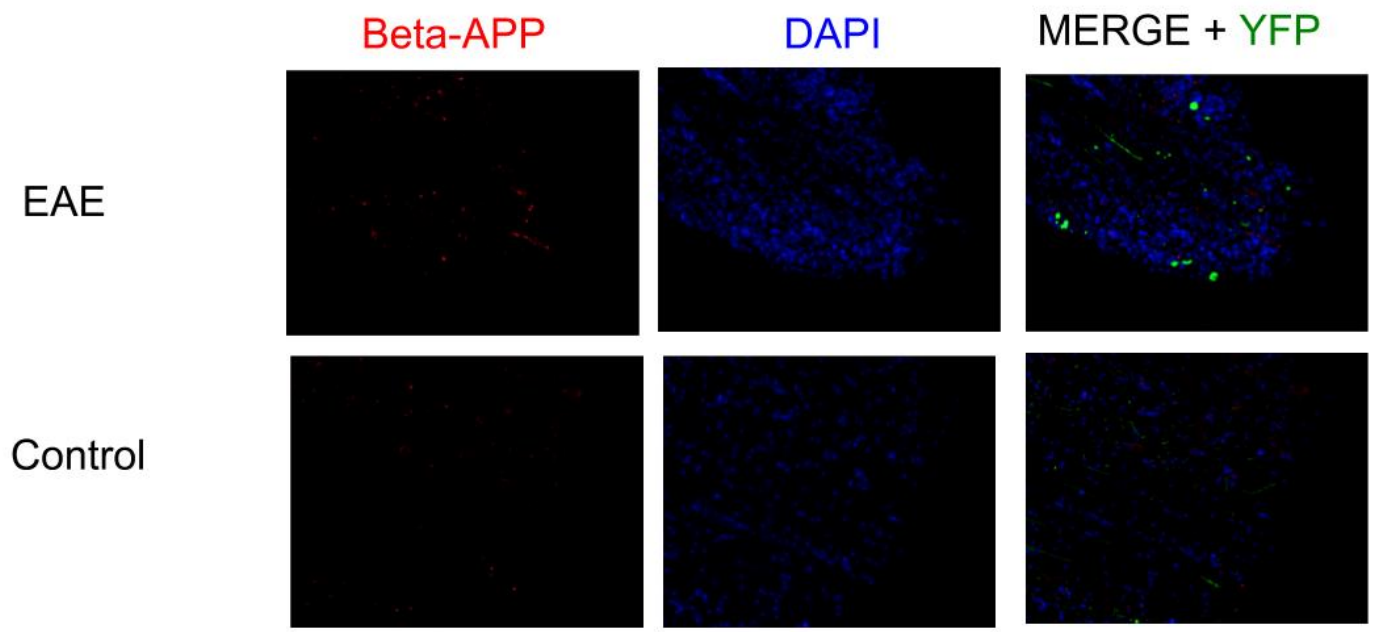

Figure 11: Increased beta-APP staining in EAE lumbar cord. Beta-APP, DAPI, and merged (+YFP) images shown. 20x magnification.

EAE in* Sarm1 *KO mice

To study the contribution of SARM1 to clinical illness, EAE was actively induced in *Sarm1* KO and WT littermates. Figure 12 shows the clinical scores for WT and *Sarm1* KO mice over a 6-week period. *Sarm1* KO mice showed comparable scores to WT littermates at the beginning of the induction but showed lower clinical scores starting around the third week. Overall, *Sarm1* KO littermates showed lower mean cumulative EAE clinical scores, although the differences were not statistically significant (Figure 12).

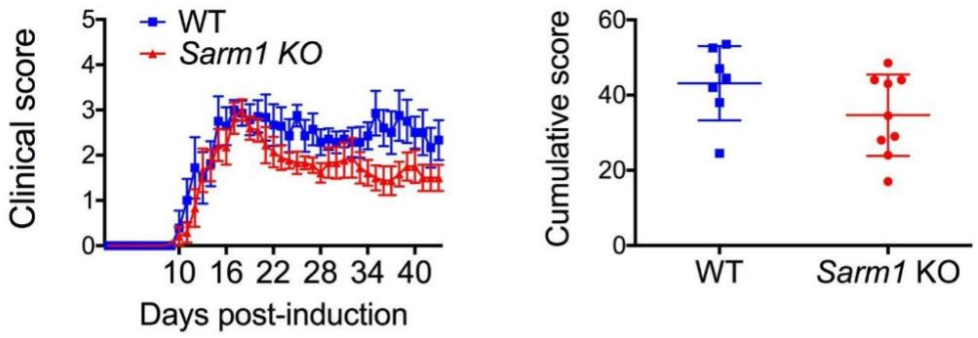

Figure 12: EAE was actively induced in *Sarm1* KO mice (N = 9) and WT littermates (N = 7). Mean clinical scores (+/- S.E.M.) for *Sarm1* KO and WT littermates (left). Mean cumulative clinical scores for *Sarm1* KO and WT littermates; lines show mean and standard deviation (right).

Beta-APP immunohistochemistry was used to assess axonal injury in *Sarm1* KO and WT mice. Beta-APP, DAPI, and multichannel images of the lumbar cord sections of WT and *Sarm1* KO mice (Figure 13). We observed that there were less Beta-APP particles in the *Sarm1* KO mouse lumbar cord then there is in WT lumbar cord (Figure 14). We found a P-value of 0.114 at a 95% confidence level. WT mice had an average of 119.7 particles per section with a standard deviation of 34.4, and *Sarm1* KO mice had an average of 67.8 particles per section with a standard deviation of 35.5.

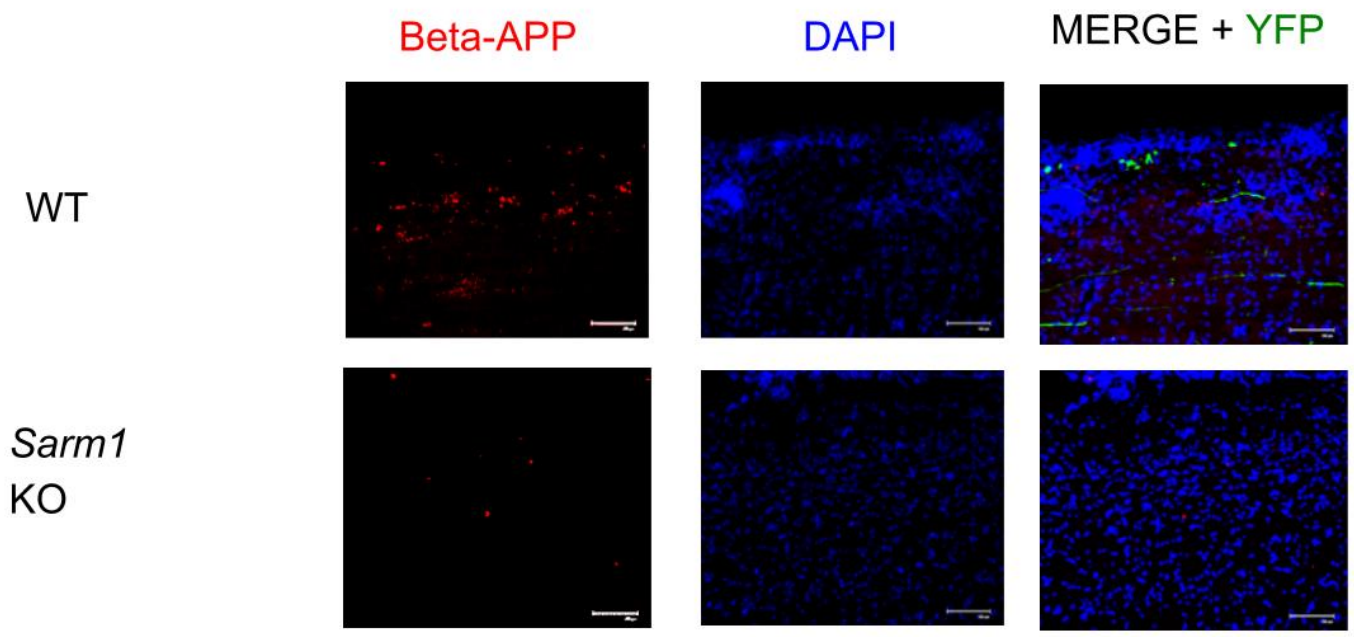

Figure 13. Decreased beta-APP staining in *Sarm1* KO lumbar cord. Beta-APP, DAPI, and merged (+YFP^{+}) images of WT and *Sarm1* KO lumbar cords shown. Scale bar = 100μm.

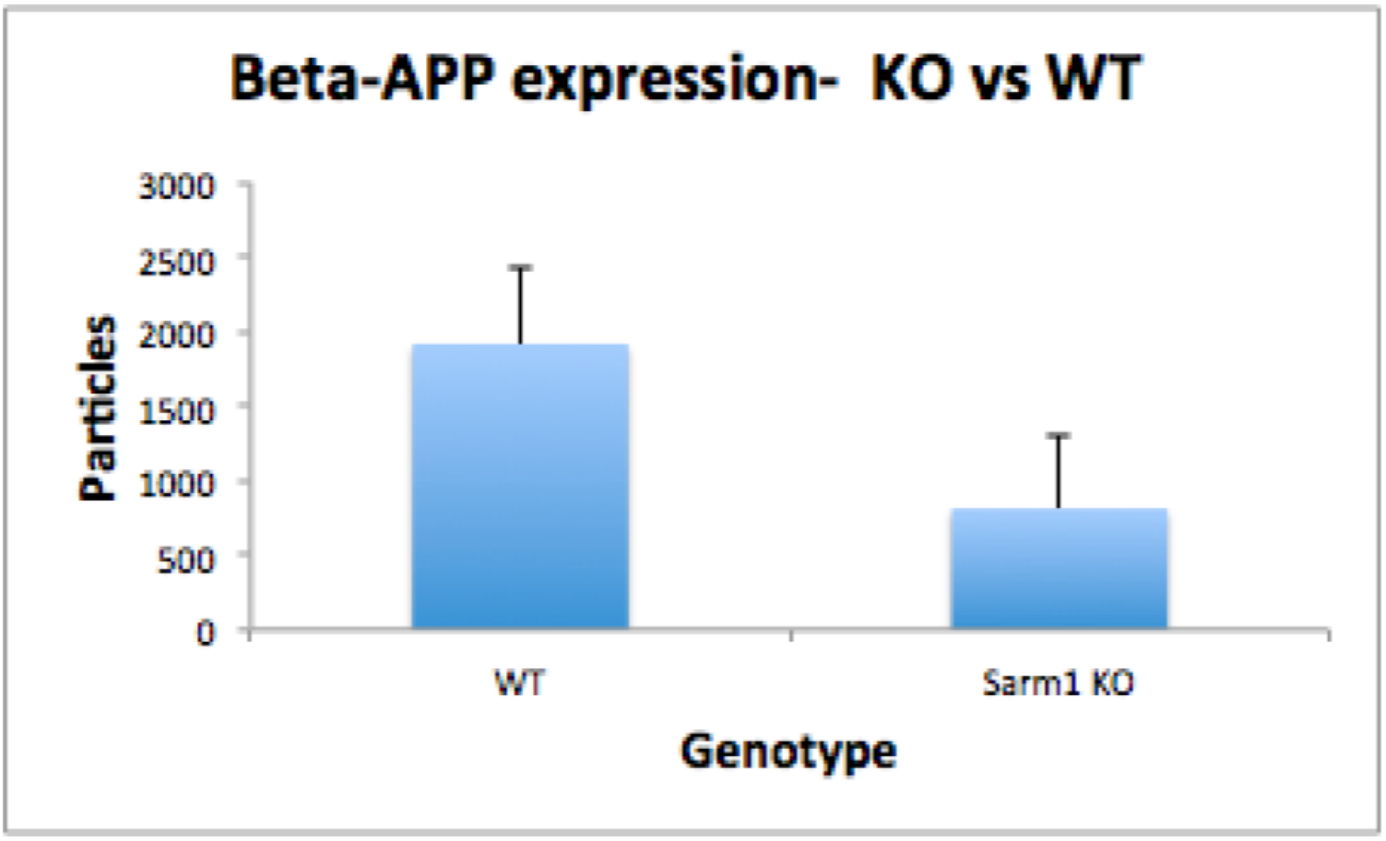

Figure 14. Beta-APP particle comparison for WT (N = 4) and *Sarm1* KO (N = 3) littermates. More Beta-APP particles were found in the WT littermates than in the *Sarm1* KO littermates. Mean (+S.E.M) shown. Mann-Whitney Test. P-value = 0.114 (W = 1).

To further assess axonal degeneration in Sarm1 KO and WT mice we generated *Sarm1* KO mice and WT littermates that were hemizygous for the YFP gene. These mice express YFP under the *Thy1* gene promoter at high levels in motor and sensory neurons, as well as subsets of central neurons. Axons were readily identified in longitudinal sections of the lumbar cord in these mice. Degenerating axons were identified by focal swelling or fragmentation. Thy-1-YFP^{+} mice sections were utilized to quantify SARM1's impact on axonal degeneration. Degrading axons

and total axons were counted. YFP, DAPI, and multichannel images of the WT and *Sarm1* KO lumbar cords are shown in Figure 15. There was a higher number of fragmented axons in WT than *Sarm1* KO mouse. Figure 16 displays the total number YFP axons in WT and *Sarm1* KO mice, which show that *Sarm1* KO mice have a lower amount of YFP expressing axons and degrading axons. We found P-values of 0.400 for total axons, 0.114 for intact axons, and 0.629 for degrading axons at a 95% confidence level. WT mice had an average of 63.9 axons per section with a standard deviation of 25.5, and *Sarm1* KO mice had an average of 44.9 axons per section with a standard deviation of 23.6.

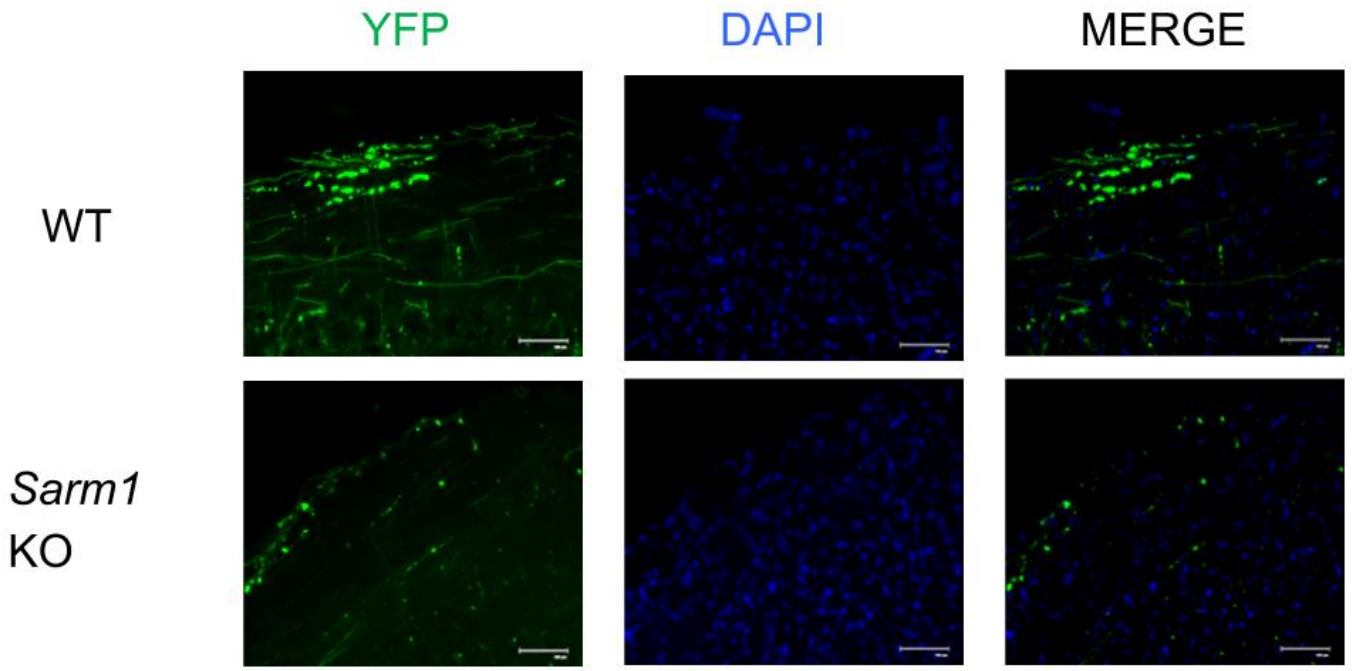

Figures 15: Decreased YFP expression and axon fragmentation in *Sarm1* KO mouse. YFP, DAPI, and merged images WT and *Sarm1* KO lumbar cord sections shown. Scale bar = 100μm.

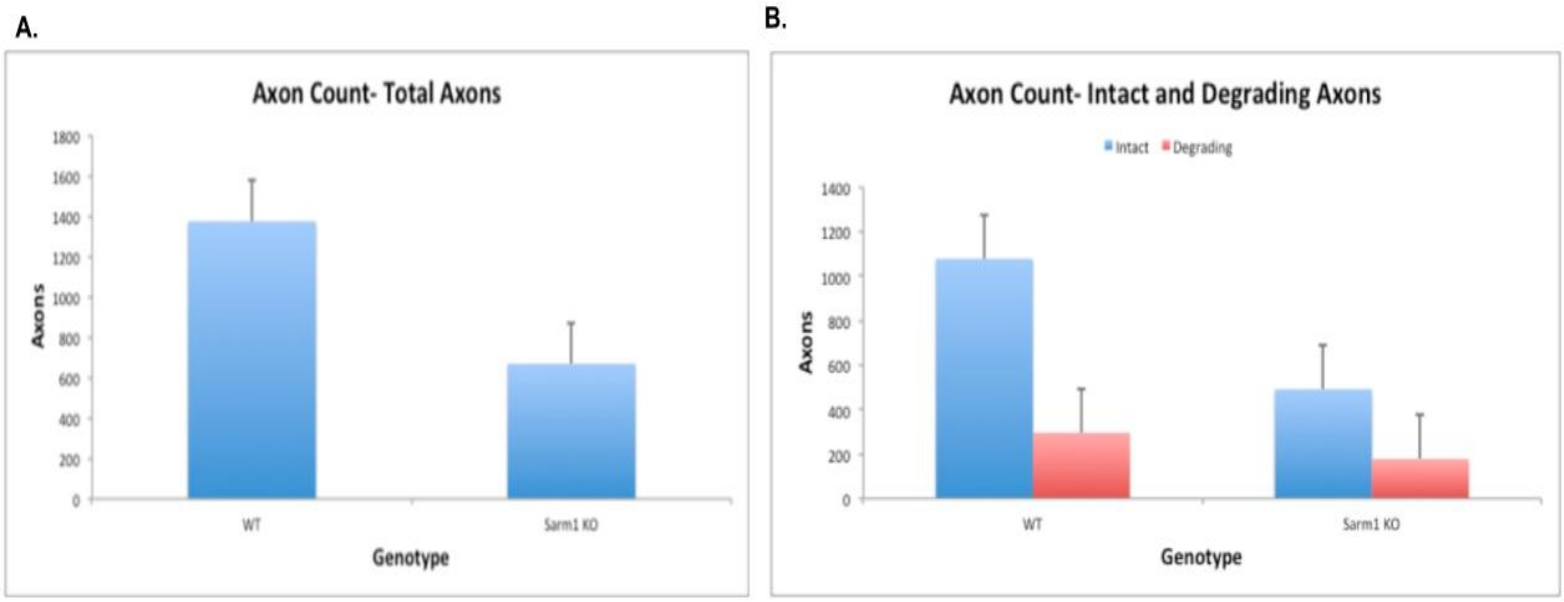

Figure 16: a) Axon counts from WT (N = 4) and *Sarm1* KO (N = 3) lumbar cord sections. More axons found in WT lumbar cords than in *Sarm1* KO lumbar cords. Mean (+S.E.M) shown. b) Intact vs. degrading axon counts from WT and *Sarm1* KO mice. Mean (+S.E.M) shown. Mann-Whitney Test. P-values: 0.400 (total) (W = 3), 0.114 (intact) (W = 3), 0.629 (degrading) (W = 8).

DISCUSSION

EAE pathology

We wanted to assess EAE pathology in mice relative to healthy mice to better understand the pathology and effects of MS. Inducing mice to have EAE has resulted in mice having higher T-cell counts in CNS tissues (84) (85). Using the T-cell marker for CD3, we were able to show that EAE induction results in higher CD3 expression (Figure 8). T-cells that infiltrate the CNS has shown to have neurodegenerative effects through targeting myelin. EAE and MS eventually result in axonal damage and dysfunction (58) (64). To assess this, we stained for phosphorylated

neurofilament H (SMI-31), dephosphorylated neurofilament H (SMI-32), and Beta-APP in EAE and healthy mice. Comparable phosphorylated neurofilament H staining was found between EAE and healthy lumbar cord (Figure 9). However, increased dephosphorylated neurofilament H staining was found with EAE induction (Figure 10). Dephosphorylated neurofilament H is a sign of poor axonal health (64). Beta-APP expression is assessed as a signifier of disrupted axonal transport in diseases such as MS and Alzheimer's. We found more Beta-APP particle expression in EAE tissue as compared to healthy tissue (Figure 11). Understanding the different ways that EAE manifest in mice was essential for establishing a baseline for SARM1. SARM1 has been studied both for its role in inflammation and axonal degeneration. Lack of SARM1 expression has been shown to protect axons (68). Mice with the *Sarm1* gene disrupted should have a starkly different pathology of EAE than those mice that don't.

SARM1 is primarily found in the brain

We first wanted to validate the genotype of SARM1 of the mice we received from Jackson Laboratory. End-point PCR was valuable in establishing the Sarm1 genotypes of several different mice. Figure 5 shows the example of a gel that was ran that had three different genotypes. Quantitative RT-PCR was performed to measure mRNA expression in various mouse body tissues. Figure 6 showed SARM1 was more expressed in the brain than in other tissues. Our data correlates to a previous study by Mink et. Al. that showed that SARM1 is highly expressed in mouse tissue (86). From previous studies, SARM1 is highly expressed in neurons and functions in neuronal death (68) (74). Assessing the expression of SARM1 in different tissues help illustrate the unique role that SARM1 has in axonal pathology. We then wanted to validate the genotype through quantitative RT-PCR using two different *Sarm1* probes (Figure 7). The neomycin cassette vector in the *Sarm1* KO mice targets and replaces exons 3-6 of the *Sarm1*

gene (91), so we aimed to compare Sarm1 expression with two different primer/probe sets that targeted different areas of the *Sarm1* gene. We found that there was less expression of *Sarm1* in the KO mouse brain with both primer/probes. Also, the primer/probe set directed against the 3' end of the *Sarm1* showed no amplification in the *Sarm1* KO brain. This data appears to be consistent with the Western Blot analysis found by Ding et. Al (91). Using qRT-PCR was helpful to assess primer quality as well as gene expression.

SARM1 and axonal degeneration

SARM1 functions to cause Wallerian degeneration through rapid NAD depletion post injury (68) (82) (88). From the clinical scores of the littermates that were induced to have EAE (Figure 12), there were comparable clinical scores between the two samples, although the SARM1 KO littermates showed improvement over time. We wanted to see if we could quantify this effect through axonal damage markers.

After staining for dephosphorylated neurofilament H (Figure 10) and Beta-APP (Figure 11), we found that the was a prominent increase in axonal damage EAE mice than in control mice. Beta-APP and dephosphorylated neurofilament H expression increase with damaged axons (89). We then wanted to see how a *Sarm1* KO EAE could reduce axonal damage as comparted to a WT EAE mouse. Thy1-YFP^{+} mice were used to quantify axonal injury in a subset of neurons that express it. We found that there was a higher number of YFP expressing axons in WT mice compared to *Sarm1* mice in total (Figure 16a) and less degrading axons in total (Figure 16b) although the p-value was not significant between the two samples. When quantifying axonal damage through B-APP, there was decreased expression in *Sarm1* KO compared to WT, although the difference was not statistically significant. Comparing the healthy lumbar cord

(Figure 11) and *Sarm1* KO (Figure 13) lumbar cord, there is some similarity in Beta-APP expression. The accuracy in counting the axons and particles can result from having a more established standard in place for counting. One way to help quantify degrading axons in the future is to establish a baseline axonal density for all sections. Comparing non-phosphorylated neurofilament H and fluoromyelin staining for *Sarm1* KO and WT lumbar cords will allow us to understand SARM1's effect on axonal damage further, while also assessing demyelination/remyelination.

Conclusions and Future Directions

We found that SARM1 is highly expressed in the brain. From there, we mainly focused on the axonal degradation effects of SARM1, showing that there is a modest, but not significant, decline in axonal injury. A future area of study is the role that SARM1 plays in cytokine production and inflammation. SARM1 activates JNK through the MKK4/MKK7 cascade and p38 through (68) (77). JNK works to enable T_H0 cells into pro-inflammatory T_H1 cells (90). SARM1 has shown to have different roles in the MAPK pathway (68) (92). SARM1 has been shown to activate ASK to phosphorylate MKK4, which goes on to activate JNK (68). Knocking out MKK4 in mice has been shown to reduce axonal degeneration (68). Pathways that could affect SARM1 can also influence inflammation, like PHR (positive regulator) and kinase AKT (negative regulator) could be researched in the context of SARM1 to clarify SARM1 impact (68). PHR loss has been shown to protect axons (68). AKT is known to be an inhibitor of MKK4 (68). On the other hand, in a study by Peng et Al., SARM1 has been shown to result in downregulation of the MAPK pathway through inhibition of TRIF and MyD88 activation of AP-

1 (92). As a result, p38 declined with SARM1 overexpression (92). Further research on the nature of SARM1 in inflammation in a different context will be critical.

Research has shown that SARM1 could function in a process called “Sarmoptosis,” which is different from apoptosis because it does not depend on caspase activation (68). This complicated process is of interest because some methods that work to prevent apoptosis, such as Bcl-XL overexpression and caspase inhibitors, do not prevent SARM-1 mediated neuronal death (68). Finding inhibitors for the pathway could be beneficial in maintaining axonal integrity. Ca^{2+} influx could be another avenue to explore as well. SARM1 is necessary for mitochondrial accumulation and subsequent dysfunction in axon metabolism (79). Also, Ca^{2+} accumulation, as stated before, result in calpain activation and cytoskeleton breakdown (52) (60) (63) (68). Using mitochondrial retention assays for calcium can help quantify this effect *in vitro*.

REFERENCES

1. Weinshenker, B. G. (1996). Epidemiology of Multiple Sclerosis. Neuroepidemiology, 14(2), 291-308. http://dx.doi.org/10.1016/S0733-8619(05)70257-7

2. Browne, P., Chandraratna, D., Angood, C., Tremlett, H., Baker, C., Taylor, B. V., & Thompson, A. J. (2014). Atlas of Multiple Sclerosis 2013: A growing global problem with widespread inequity. Neurology, 83(11), 1022-1024. doi:10.1212/wnl.0000000000000768

3. Naci, Huseyin, et al. "Economic Burden of Multiple Sclerosis." PharmacoEconomics, vol. 28, no. 5, 2010, pp. 363–379., doi:10.2165/11532230-000000000-00000.

4. Ernstsson, O., Gyllensten, H., Alexanderson, K., Tinghög, P., Friberg, E., & Norlund, A. (2016, July 13). Cost of Illness of Multiple Sclerosis - A Systematic Review. Retrieved November 12, 2017, from http://journals.plos.org/plosone/article?id=10.1371%2Fjournal.pone.0159129#references

5. PhD, R. A., MSc, L. E., MSc, J. M., Cossoy, M. M., PhD, J. B., & And, S. L. (2015, July 21). Effect of comorbidity on mortality in multiple sclerosis. Retrieved November 14, 2017, from http://www.neurology.org/content/85/3/240.full

6. Lunde HB, Assmus J, Kjell-Morten M, et al Survival and cause of death in multiple sclerosis: a 60-year longitudinal population study J Neurol Neurosurg Psychiatry Published Online First: 01 April 2017. doi: 10.1136/jnnp-2016-315238

7. Leray E, Vukusic S, Debouverie M, Clanet M, Brochet B, et al. (2015) Excess Mortality in Patients with Multiple Sclerosis Starts at 20 Years from Clinical Onset: Data from a Large-Scale French Observational Study. PLOS ONE 10(7): e0132033. https://doi.org/10.1371/journal.pone.0132033

8. Cook, S. D. (2006). Multiple Sclerosis: An autoimmune Disease of the Central Nervous System? In Handbook of Multiple Sclerosis(4th ed., pp. 97-107). New York, NY: Taylor and Francis Group.

9. Cook, S. D. (2006). Multiple Sclerosis: Evidence for an Infectious Etiology of Multiple Sclerosis. In Handbook of Multiple Sclerosis (4th ed., pp. 73-82). New York, NY: Taylor and Francis Group.

10. Trapp, Bruce D., Richard Ransohoff, and Richard Rudick. "Axonal pathology in multiple sclerosis: relationship to neurologic disability." Current Opinion in Neurology 12, no. 3 (1999): 295-302. Accessed November 03, 2017. doi:10.1097/00019052-199906000-00008.

11. Raff, M. C., Whitmore, A. V., & Finn, J. T. (2002). Axonal Self-Destruction and Neurodegeneration. Science, 296(5569), 868-871. doi:10.1126/science.1068613

12. Pollard, J. (2017). Multiple Sclerosis. Retrieved November 09, 2017, from http://brainfoundation.org.au/disorders/multiple-sclerosis

13. Hauser, S. L., & Oksenberg, J. R. (2006). The Neurobiology of Multiple Sclerosis: Genes, Inflammation, and Neurodegeneration. Neuron, 52(1), 61-76. doi:10.1016/j.neuron.2006.09.011

14. Lorefice, L., Fenu, G., Sardu, C., Frau, J., Coghe, G., Costa, G., . . . Cocco, E. (2017). Multiple sclerosis and HLA genotypes: A possible influence on brain atrophy. Multiple Sclerosis Journal, 135245851773998. doi:10.1177/1352458517739989

15. Dyment, D. A., Sadnovich, A. D., & Ebers, G. C. (1997, September 01). Genetics of Multiple Sclerosis | Human Molecular Genetics | Oxford Academic. Retrieved November 13, 2017, from https://academic.oup.com/hmg/article/6/10/1693/587516#9539951

16. Comabella, M., Craig, D. W., Camiña-Tato, M., Morcillo, C., Lopez, C., Navarro, A., . . . Martin, R. (2008, October 22). Identification of a Novel Risk Locus for Multiple Sclerosis at 13q31.3 by a Pooled Genome-Wide Scan of 500,000 Single Nucleotide Polymorphisms. Retrieved November 12, 2017, from http://journals.plos.org/plosone/article?id=10.1371%2Fjournal.pone.0003490

17. Willer, C. J., Dyment, D. A., Risch, N. J., Sadovnick, A. D., & Ebers, G. C. (2003). Twin concordance and sibling recurrence rates in multiple sclerosis. Proceedings of the National Academy of Sciences, 100(22), 12877-12882. doi:10.1073/pnas.1932604100

18. Wingerchuk, D. M. (2011). Environmental Factors in Multiple Sclerosis: Epstein-Barr Virus, Vitamin D, and Cigarette Smoking. Mount Sinai Journal of Medicine: A Journal of Translational and Personalized Medicine, 78(2), 221-230. doi:10.1002/msj.20240

19. Ascherio, A. and Munger, K. L. (2007), Environmental risk factors for multiple sclerosis. Part II: Noninfectious factors. Ann Neurol., 61: 504–513. doi:10.1002/ana.21141

20. Kingwell, E., Marriott, J. J., Jetté, N., Pringsheim, T., Makhani, N., Morrow, S. A., … Marrie, R. A. (2013). Incidence and prevalence of multiple sclerosis in Europe: a systematic review. BMC Neurology, 13, 128. http://doi.org/10.1186/1471-2377-13-128

21. Khan, O., Williams, M. J., Amezcua, L., Javed, A., Larsen, K. E., & Smrtka, J. M. (2015). Multiple sclerosis in US minority populations: Clinical practice insights. Neurology: Clinical Practice, 5(2), 132–142. http://doi.org/10.1212/CPJ.0000000000000112

22. Polman, C. H., Reingold, S. C., Banwell, B., Clanet, M., Cohen, J. A., Filippi, M., … Wolinsky, J. S. (2011). Diagnostic criteria for multiple sclerosis: 2010 Revisions to the McDonald criteria. Annals of Neurology, 69(2), 292–302. http://doi.org/10.1002/ana.2236

23. Cook, S. D. (2006). Multiple Sclerosis: An autoimmune Disease of the Central Nervous System? In Handbook of Multiple Sclerosis(4th ed., pp. 153-158). New York, NY: Taylor and Francis Group.

24. Thompson AJ, SYMPTOMATIC MANAGEMENT AND REHABILITATION IN MULTIPLE SCLEROSIS, Journal of Neurology, Neurosurgery & Psychiatry 2001;71:ii22-ii27.

25. Multiple Sclerosis: New Insights and Trends, M. Inglese, American Journal of Neuroradiology May 2006, 27 (5) 954-957

26. Marcus, J. F., & Waubant, E. L. (2013). Updates on Clinically Isolated Syndrome and Diagnostic Criteria for Multiple Sclerosis. The Neurohospitalist, 3(2), 65–80. http://doi.org/10.1177/1941874412457183

27. Palace J , MAKING THE DIAGNOSIS OF MULTIPLE SCLEROSIS, Journal of Neurology, Neurosurgery & Psychiatry 2001;71:ii3-ii8.

28. Types of MS and MS Treatment Options—multiplesclerosis.com. (n.d.). Retrieved November 14, 2017, from https://www.multiplesclerosis.com/us/treatment.php

29. Multiple Sclerosis. (n.d.). Retrieved November 14, 2017, from http://premierneurologycenter.com/education/multiple-sclerosis/

30. Holland, N. J., Schneider, D. M., Rapp, R., & Kalb, R. C. (2011). Meeting the Needs of People with Primary Progressive Multiple Sclerosis, Their Families, and the Health-Care Community. International Journal of MS Care, 13(2), 65–74. http://doi.org/10.7224/1537-2073-13.2.65

31. Shaik Ahmed Sanai, Vasu Saini, Ralph HB Benedict, Robert Zivadinov, Barbara E Teter, Murali Ramanathan, Bianca Weinstock-Guttman, Aging and multiple sclerosis, Multiple Sclerosis Journal, Vol 22, Issue 6, pp. 717 – 725, First Published February 19, 2016, https://doi.org/10.1177/1352458516634871

32. Cook, S. D. (2006). Multiple Sclerosis: An autoimmune Disease of the Central Nervous System? In Handbook of Multiple Sclerosis(4th ed., pp. 177-208). New York, NY: Taylor and Francis Group.

33. Cennamo, G., Romano, M. R., Vecchio, E. C., Minervino, C., della Guardia, C., Velotti, N., … Cennamo, G. (2016). Anatomical and functional retinal changes in multiple sclerosis. Eye, 30(3), 456–462. http://doi.org/10.1038/eye.2015.256

34. Peterson, L. K., & Fujinami, R. S. (2007). Inflammation, Demyelination, Neurodegeneration and Neuroprotection in the Pathogenesis of Multiple Sclerosis. Journal of Neuroimmunology, 184(1-2), 37–44. http://doi.org/10.1016/j.jneuroim.2006.11.015

35. Kebir, H., Kreymborg, K., Ifergan, I., Dodelet-Devillers, A., Cayrol, R., Bernard, M., … Prat, A. (2007). Human TH17 lymphocytes promote blood-brain barrier disruption and central nervous system inflammation. Nature Medicine, 13(10), 1173–1175. http://doi.org/10.1038/nm1651

36. Huseby, E. S., Huseby, P. G., Shah, S., Smith, R., & Stadinski, B. D. (2012). Pathogenic CD8 T Cells in Multiple Sclerosis and Its Experimental Models. Frontiers in Immunology, 3, 64. http://doi.org/10.3389/fimmu.2012.00064

37. Wekerle, H. (2017). B cells in multiple sclerosis. Autoimmunity, 50(1), 57-60. doi:https://doi.org/10.1080/08916934.2017.1281914

38. Lehmann-Horn, K., Kronsbein, H. C., & Weber, M. S. (2013). Targeting B cells in the treatment of multiple sclerosis: recent advances and remaining challenges. Therapeutic Advances in Neurological Disorders, 6(3), 161–173. http://doi.org/10.1177/1756285612474333

39. Correale, J., & Farez, M. F. (2015). The Role of Astrocytes in Multiple Sclerosis Progression. Frontiers in Neurology, 6, 180. http://doi.org/10.3389/fneur.2015.00180

40. Luo, C., Jian, C., Liao, Y., Huang, Q., Wu, Y., Liu, X., … Wu, Y. (2017). The role of microglia in multiple sclerosis. Neuropsychiatric Disease and Treatment, 13, 1661–1667. http://doi.org/10.2147/NDT.S140634

41. Tanja Kuhlmann, Gueanelle Lingfeld, Andreas Bitsch, Jana Schuchardt, Wolfgang Brück; Acute axonal damage in multiple sclerosis is most extensive in early disease stages and decreases over time, Brain, Volume 125, Issue 10, 1 October 2002, Pages 2202–2212, https://doi.org/10.1093/brain/awf235

42. Ludwin, S. K., Rao, V. T., Moore, C. S., & Antel, J. P. (2016). Astrocytes in multiple sclerosis. Multiple Sclerosis Journal, 22(9), 1114-1124. doi:10.1177/1352458516643396

43. Rao P., Segal B.M. (2012) Experimental Autoimmune Encephalomyelitis. In: Perl A. (eds) Autoimmunity. Methods in Molecular Biology (Methods and Protocols), vol 900. Humana Press, Totowa, NJ. https://doi.org/10.1007/978-1-60761-720-4_18

44. Manuel A. Friese, Lars Fugger; T cells and microglia as drivers of multiple sclerosis pathology, Brain, Volume 130, Issue 11, 1 November 2007, Pages 2755–2757, https://doi.org/10.1093/brain/awm246

45. Miron, V. E., Boyd, A., Zhao, J.-W., Yuen, T. J., Ruckh, J. M., Shadrach, J. L., … ffrench-Constant, C. (2013). M2 microglia/macrophages drive oligodendrocyte differentiation during CNS remyelination. Nature Neuroscience, 16(9), 1211–1218. http://doi.org/10.1038/nn.3469

46. Robert T. Naismith, Anne H. Cross; Enhancing our understanding of white matter changes in early multiple sclerosis, Brain, Volume 138, Issue 9, 1 September 2015, Pages 2465–2466, https://doi.org/10.1093/brain/awv196

47. N. Joan Abbott, Adjanie A.K. Patabendige, Diana E.M. Dolman, Siti R. Yusof, David J. Begley, Structure and function of the blood–brain barrier, In Neurobiology of Disease, Volume 37, Issue 1, 2010, Pages 13-25, ISSN 0969-9961, https://doi.org/10.1016/j.nbd.2009.07.030

48. Takeshita, Y., & Ransohoff, R. M. (2012). Inflammatory cell trafficking across the blood-brain barrier (BBB): Chemokine regulation and in vitro models. Immunological Reviews, 248(1), 228–239. http://doi.org/10.1111/j.1600-065X.2012.01127.x

49. Helga E. de Vries, Johan Kuiper, Albertus G. de Boer, Theo J. C. Van Berkel and Douwe D. Breimer, The Blood-Brain Barrier in Neuroinflammatory Diseases, Pharmacological Reviews June 1, 1997, 49 (2) 143-156;

50. Popescu BFG, Pirko I, Lucchinetti CF. Pathology of Multiple Sclerosis: Where Do We Stand? Continuum : Lifelong Learning in Neurology. 2013;19(4 Multiple Sclerosis):901-921. doi:10.1212/01.CON.0000433291.23091.65.

51. Aditya G. Shivane, Arundhati Chakrabarty, Multiple sclerosis and demyelination, Current Diagnostic Pathology,Volume 13,Issue 3, 2007, Pages 193-202,ISSN 0968-6053, https://doi.org/10.1016/j.cdip.2007.04.003

52. Cook, S. D. (2006). Multiple Sclerosis: Pathology: What May It Tell Us? In Handbook of Multiple Sclerosis(4th ed., pp. 115-151) New York, NY: Taylor and Francis Group.

53. Filippi, M., Rovaris, M., & Comi, G. (2007). Neurodegeneration in multiple sclerosis (1st ed.). Milan, Italy: Springer. doi:10.1007/978-88-470-0391-0

54. Wu, G. F., & Alvarez, E. (2011). The immuno-pathophysiology of multiple sclerosis. Neurologic Clinics, 29(2), 257–278. http://doi.org/10.1016/j.ncl.2010.12.009

55. Alexandra Kutzelnigg, Claudia F. Lucchinetti, Christine Stadelmann, Wolfgang Brück, Helmut Rauschka, Markus Bergmann, Manfred Schmidbauer, Joseph E. Parisi, Hans Lassmann; Cortical demyelination and diffuse white matter injury in multiple sclerosis, Brain, Volume 128, Issue 11, 1 November 2005, Pages 2705–2712, https://doi.org/10.1093/brain/awh641

56. Podbielska M, Banik NL, Kurowska E, Hogan EL. Myelin Recovery in Multiple Sclerosis: The Challenge of Remyelination. Brain Sciences. 2013;3(3):1282-1324. doi:10.3390/brainsci3031282.

57. Brück, Wolfgang et al, Remyelination in multiple sclerosis, Journal of the Neurological Sciences , Volume 206 , Issue 2 , 181 - 185 doi: https://doi.org/10.1016/S0022-510X(02)00191-0

58. A. Bitsch, J. Schuchardt, S. Bunkowski, T. Kuhlmann, W. Brück; Acute axonal injury in multiple sclerosis: Correlation with demyelination and inflammation, Brain, Volume 123, Issue 6, 1 June 2000, Pages 1174–1183, https://doi.org/10.1093/brain/123.6.1174

59. Petrova, N., Carassiti, D., Altmann, D. R., Baker, D. and Schmierer, K. (2017), Axonal loss in the multiple sclerosis spinal cord revisited. Brain Pathology. doi:10.1111/bpa.12516

60. Barbara Kornek, Maria K. Storch, Jan Bauer, Atbin Djamshidian, Robert Weissert, Erik Wallstroem, Andreas Stefferl, Fritz Zimprich, Tomas Olsson, Christopher Linington, Manfred Schmidbauer, Hans Lassmann; Distribution of a calcium channel subunit in dystrophic axons in multiple sclerosis and experimental autoimmune encephalomyelitis, Brain, Volume 124, Issue 6, 1 June 2001, Pages 1114–1124, https://doi.org/10.1093/brain/124.6.1114

61. Haines, J. D., Inglese, M., & Casaccia, P. (2011). Axonal Damage in Multiple Sclerosis. The Mount Sinai Journal of Medicine, New York, 78(2), 231–243. http://doi.org/10.1002/msj.20246

62. Trapp, B. D., Peterson, J., Ransohoff, R. M., Rudick, R., Mörk, S., & Bö, L. (1998). Axonal Transection in the Lesions of Multiple Sclerosis [Abstract]. The New England Journal of Medicine, 338(5), 278-285. doi:10.1056/NEJM199801293380502

63. Werner, P., Pitt, D. and Raine, C. S. (2001), Multiple sclerosis: Altered glutamate homeostasis in lesions correlates with oligodendrocyte and axonal damage. Ann Neurol., 50: 169–180. doi:10.1002/ana.1077

64. Shermali Gunawardena, Lawrence S.B. Goldstein, Disruption of Axonal Transport and Neuronal Viability by Amyloid Precursor Protein Mutations in Drosophila, In Neuron, Volume 32, Issue 3, 2001, Pages 389-401, ISSN 0896-6273, https://doi.org/10.1016/S0896-6273(01)00496-2.(http://www.sciencedirect.com/science/article/pii/S0896627301004962)

65. Chiba, K., Araseki, M., Nozawa, K., Furukori, K., Araki, Y., Matsushima, T., … Suzuki, T. (2014). Quantitative analysis of APP axonal transport in neurons: role of JIP1 in enhanced APP anterograde transport. Molecular Biology of the Cell, 25(22), 3569–3580. http://doi.org/10.1091/mbc.E14-06-1111

66. Aidong Yuan, Mala V. Rao, Veeranna, Ralph A. Nixon, Neurofilaments at a glance, J Cell Sci 2012 125: 3257-3263; doi: 10.1242/jcs.104729

67. Cook, S. D. (2006). Multiple Sclerosis: An autoimmune Disease of the Central Nervous System? In Handbook of Multiple Sclerosis(4th ed., pp. 231-238). New York, NY: Taylor and Francis Group.

68. Josiah Gerdts, Daniel W. Summers, Jeffrey Milbrandt, Aaron DiAntonio, Axon Self-Destruction: New Links among SARM1, MAPKs, and NAD+ Metabolism, In Neuron, Volume 89, Issue 3, 2016, Pages 449-460, ISSN 0896-6273, https://doi.org/10.1016/j.neuron.2015.12.023.(http://www.sciencedirect.com/science/article/pii/S0896627315011253)

69. Coleman, M. (2005). Axon degeneration mechanisms: Commonality amid diversity. Nature Reviews Neuroscience, 6(11), 889-898. doi:10.1038/nrn1788

70. Di Stefano, M., Nascimento-Ferreira, I., Orsomando, G., Mori, V., Gilley, J., Brown, R., … Conforti, L. (2015). A rise in NAD precursor nicotinamide mononucleotide (NMN) after injury promotes axon degeneration. Cell Death and Differentiation, 22(5), 731–742. http://doi.org/10.1038/cdd.2014.164

71. Coleman, M. P., & Freeman, M. R. (2010). Wallerian Degeneration, WldS, and Nmnat. Annual Review of Neuroscience, 33, 245–267. http://doi.org/10.1146/annurev-neuro-060909-153248

72. Gaudet, A. D., Popovich, P. G., & Ramer, M. S. (2011). Wallerian degeneration: Gaining perspective on inflammatory events after peripheral nerve injury. *Journal of Neuroinflammation, 8*(1), 110. doi:10.1186/1742-2094-8-110

73. Peng, J. , Yuan, Q. , Lin, B. , Panneerselvam, P. , Wang, X. , Luan, X. L., Lim, S. K., Leung, B. P., Ho, B. and Ding, J. L. (2010), SARM inhibits both TRIF- and MyD88-mediated AP-1 activation. Eur. J. Immunol., 40: 1738-1747. doi:10.1002/eji.200940034

74. Kim, Y., Zhou, P., Qian, L., Chuang, J.-Z., Lee, J., Li, C., … Ding, A. (2007). MyD88-5 links mitochondria, microtubules, and JNK3 in neurons and regulates neuronal survival. The Journal of Experimental Medicine, 204(9), 2063–2074. http://doi.org/10.1084/jem.20070868

75. Matyas Mink, Ben Fogelgren, Krzysztof Olszewski, Peter Maroy, Katalin Csiszar, A Novel Human Gene (SARM) at Chromosome 17q11 Encodes a Protein with a SAM Motif and Structural Similarity to Armadillo/β-Catenin That Is Conserved in Mouse, Drosophila, and Caenorhabditis elegans, Genomics, Volume 74, Issue 2,2001,Pages 234-244,ISSN 0888-7543, https://doi.org/10.1006/geno.2001.6548.

76. Massoll, C., Mando, W., & Chintala, S. K. (2013). Excitotoxicity Upregulates SARM1 Protein Expression and Promotes Wallerian-Like Degeneration of Retinal Ganglion Cells and Their Axons. Investigative Ophthalmology & Visual Science, 54(4), 2771–2780. http://doi.org/10.1167/iovs.12-10973

77. Dalod, M. (2007). Studies of SARM1 Uncover Similarities Between Immune and Neuronal Responses to Danger. Sciences STKE, 2007(417). doi:10.1126/stke.4172007pe73

78. Yang, Jing et al., Pathological Axonal Death through a MAPK Cascade that Triggers a Local Energy Deficit. Cell , Volume 160 , Issue 1 , 161 – 176, https://doi.org/10.1016/j.cell.2014.11.053

79. Mukherjee, P., Winkler, C. W., Taylor, K. G., Woods, T. A., Nair, V., Khan, B. A., & Peterson, K. E. (2015). SARM1, not MyD88, mediates TLR7/TLR9-induced apoptosis in neurons. Journal of Immunology (Baltimore, Md. : 1950), 195(10), 4913–4921. http://doi.org/10.4049/jimmunol.1500953

80. Szretter, K. J., Samuel, M. A., Gilfillan, S., Fuchs, A., Colonna, M., & Diamond, M. S. (2009). The Immune Adaptor Molecule SARM Modulates Tumor Necrosis Factor Alpha Production and Microglia Activation in the Brainstem and Restricts West Nile Virus Pathogenesis. Journal of Virology, 83(18), 9329-9338. doi:10.1128/jvi.00836-09

81. Lin, C., Liu, H., Chen, C., & Hsueh, Y. (2013). Neuronally-expressed Sarm1 regulates expression of inflammatory and antiviral cytokines in brains. Innate Immunity, 20(2), 161-172. doi:10.1177/1753425913485877

82. Gerdts, J., Brace, E. J., Sasaki, Y., DiAntonio, A., & Milbrandt, J. (2015). SARM1 activation triggers axon degeneration locally via NAD+ destruction. Science (New York, N.Y.), 348(6233), 453–457. http://doi.org/10.1126/science.1258366

83. Constantinescu, C. S., Farooqi, N., O'Brien, K., & Gran, B. (2011). Experimental autoimmune encephalomyelitis (EAE) as a model for multiple sclerosis (MS). British Journal of Pharmacology, 164(4), 1079–1106. http://doi.org/10.1111/j.1476-5381.2011.01302.x

84. Daniel C. Bullard, Xianzhen Hu, Trenton R. Schoeb, Robert G. Collins, Arthur L. Beaudet, Scott R. Barnum, Intercellular Adhesion Molecule-1 Expression Is Required on Multiple Cell Types for the Development of Experimental Autoimmune Encephalomyelitis. The Journal of Immunology January 15, 2007, 178 (2) 851-857; DOI: 10.4049/jimmunol.178.2.851

85. Herbert P. M. Brok, Marjan van Meurs, Erwin Blezer, Allen Schantz, David Peritt, George Treacy, Jon D. Laman, Jan Bauer, Bert A. 't Hart, Prevention of Experimental Autoimmune Encephalomyelitis in Common Marmosets Using an Anti-IL-12p40 Monoclonal Antibody, The Journal of Immunology December 1, 2002, 169 (11) 6554-6563; DOI: 10.4049/jimmunol.169.11.6554

86. Sarm1 MGI Mouse Gene Detail - MGI:2136419 - sterile alpha and HEAT/Armadillo motif containing 1. (n.d.). Retrieved April 19, 2018, from http://www.informatics.jax.org/marker/MGI:2136419

87. Schindelin, J.; Arganda-Carreras, I. & Frise, E. et al. (2012), "Fiji: an open-source platform for biological-image analysis", Nature methods 9(7): 676-682, PMID 22743772, doi:10.1038/nmeth.2019 (on Google Scholar).

88. Summers, D. W., Gibson, D. A., DiAntonio, A., & Milbrandt, J. (2016). SARM1-specific motifs in the TIR domain enable NAD+ loss and regulate injury-induced SARM1

activation. Proceedings of the National Academy of Sciences of the United States of America, 113(41), E6271–E6280. http://doi.org/10.1073/pnas.1601506113

89. Mangiardi, M., Crawford, D. K., Xia, X., Du, S., Simon-Freeman, R., Voskuhl, R. R., & Tiwari-Woodruff, S. K. (2011). An Animal Model of Cortical and Callosal Pathology in Multiple Sclerosis. Brain Pathology (Zurich, Switzerland), 21(3), 263–278. http://doi.org/10.1111/j.1750-3639.2010.00444.x

90. Rana A. K. Singh, Jingwu Z. Zhang Differential Activation of ERK, p38, and JNK Required for Th1 and Th2 Deviation in Myelin-Reactive T Cells Induced by Altered Peptide Ligand, The Journal of Immunology December 15, 2004, 173 (12) 7299-7307; DOI: 10.4049/jimmunol.173.12.7299

91. Hou Y-J, Banerjee R, Thomas B, et al. SARM is Required for Neuronal Injury and Cytokine Production in Response to Central Nervous System Viral Infection. *Journal of immunology (Baltimore, Md : 1950)*. 2013;191(2):875-883. doi:10.4049/jimmunol.1300374.

92. Peng, J., Yuan, Q., Lin, B., Panneerselvam, P., Wang, X., Luan, X. L., … Ding, J. L. (2010). SARM inhibits both TRIF- and MyD88-mediated AP-1 activation. European Journal of Immunology, 40(6), 1738–1747. https://doi.org/10.1002/eji.200940034

VITA

Daniel Chikamnele Njoku was born on May 1, 1993 in Norfolk, VA, but moved to Central Virginia at the age of 6. After graduating from high school in 2011, Daniel matriculated to Cornell University. Daniel graduated with a B.A. degree in Chemistry and Chemical Biology in 2015. After graduated, Daniel took graduate courses at VCU School of Medicine and began to shadow doctors. Daniel then earned a certificate for the Premedical Graduated Health Sciences Certificate Program at VCU in 2017. Daniel then worked on earning a M.S in Physiology and Biophysics at VCU under Dr. Unsong Oh. While working on his Master's, Daniel was a medical scribe in Summer 2017. He also volunteered at Church Hill Activities and Tutoring, the Medical Reserve Corps of Virginia, and for Ronald McDonald House Charities of Richmond. He was also a tutor for graduate Physiology, Histology, and Biochemistry for the VCU Division for Academic Success. After earning his M.S. degree, Daniel will pursue an M.D. degree at VCU starting in Fall 2018.